AD-A067 909 NORTHWESTERN UNIV EVANSTON IL DEPT OF MATERIALS SCIENCE F/G 11/6
INFLUENCE OF MULTIAXIAL STRESS STATES, STRESS GRADIENTS AND ELA--ETC(U)
APR 79 H DOELLE N00014-75-C-0580
UNCLASSIFIED TR-22 NL

END
DATE FILMED
6-79
DDC

LEVEL II (13)

NORTHWESTERN UNIVERSITY

DEPARTMENT OF MATERIALS SCIENCE

Technical Report No. 22

(11) 12 April 1979

(12) 52p.

(15) Office of Naval Research
Contract N00014-75-C-0580
NR 031-733

(6) INFLUENCE OF MULTIAXIAL STRESS STATES, STRESS GRADIENTS AND ELASTIC ANISOTROPY ON THE EVALUATION OF (RESIDUAL) STRESSES BY X-RAYS.

by

H. Dölle

(10) H. Doelle

(9) Technical rept.

(14) TR-22

EVANSTON, ILLINOIS

260 810 Jur

INFLUENCE OF MULTIAXIAL STRESS STATES, STRESS GRADIENTS AND ELASTIC ANISOTROPY ON THE EVALUATION OF (RESIDUAL) STRESSES BY X-RAYS

by H. Dölle

Dept. of Materials Science and Engineering
The Technological Institute
Northwestern University
Evanston, IL. 60201 U.S.A.

Abstract

In recent years nonlinear d vs. $\sin^2\psi$-distributions have been observed in stressed materials, which cannot be explained by the classical fundamentals of X-ray stress measurement. d- is the interplanar spacing measured and ψ is the angle between the surface normal of the sample and the measuring direction. This paper reviews treatments for these nonlinear distributions, including stress gradients, shear-stresses and anisotropic X-ray elastic constants. Methods for the evaluation of stresses are reported, and recommendations are given for the practical application of X-ray stress measurement.

1. Introduction

The X-ray method for determining residual or applied stresses in crystalline materials is based on the measurement of interplanar spacings "d" at various tilts, φ and ψ to the X-ray beam, see Fig. 1. In a polycrystalline specimen, only those grains properly oriented to diffract at each tilt contribute to the diffraction profile. This selectivity implies that the elastic constants connecting the measured strains (or change in interplanar spacings)

to the stresses will vary with the particular set of (hkℓ) planes chosen for measurement. A recent review of this problem is contained in references (Marion and Cohen, 1977; Macherauch and Wolfstieg, 1977). At this point in time, theory (Bollen rath, Hauk and Müller, 1967) allows for an anisotropic grain coupled to an isotropic matrix and the variation in X-ray elastic constants (REC) with crystallographic direction match reasonably well with measured values (Macherauch and Wolfstieg, 1977). However, their large change with plastic tensile deformation found by Taira, Hayashi and Watase (1968), Marion and Cohen (1977) and by Dölle, Hauk, Kloth, Over, and Wichert (1977), is not yet understood.

Recently, there have been some unusual phenomena found in X-ray stress measurements suggesting that extensions of the theoretical background might permit an understanding of these new experimental results, particularly for textured materials and for materials deformed by large stresses tangent to the surface. From the theory of isotropic elasticity, with d_o as the lattice parameter of the unstressed material (Macherauch and Müller, 1961; Barrett and Massalski, 1966),

$$\frac{d_{\varphi\psi} - d_o}{d_o} = \tfrac{1}{2}\, s_2(hk\ell)\cdot[\sigma_1\cdot\cos^2\varphi + \sigma_2\cdot\sin^2\varphi]\cdot\sin^2\psi + s_1(hk\ell)\cdot[\sigma_1 + \sigma_2] \qquad (1)$$

with the principal stresses σ_1 and σ_2 and the X-ray elastic constants (REC)

$$\tfrac{1}{2}\, s_2(hk\ell) = \left(\frac{1+\nu}{E}\right)^{hk\ell};\ s_1(hk\ell) = \left(-\frac{\nu}{E}\right)^{hk\ell}. \qquad (2a,b)$$

According to equation (1), $d_{\varphi\psi}$ should be linear with $\sin^2\psi$, but it has recently been found that different d-$\sin^2\psi$ curves occur for positive and negative ψ (see Fig. 2a) after grinding (Walburger, 1973; Faninger and Walburger, 1976; Wolfstieg and

Macherauch, 1976; Macherauch and Wolfstieg, 1977), or rolling friction (Christ and Krause, 1975, Krause and Jühe, 1976) or wear (Krause and Jühe, 1977) and oscillation (see Fig. 2b) may occur in textured materials (Bollenrath, Hauk and Weidemann, 1967; Shiraiwa and Sakamoto, 1970, Marion and Cohen, 1975; Hauk, Herlach and Sesemann, 1975). Since the penetration depth of X-rays depend on ψ (Wolfstieg, 1976), strong gradients can cause additional nonlinearities (Shiraiwa and Sakamoto, 1972).

It is the purpose of this paper to summarize the recent theoretical approaches taken by Shiraiwa and Sakamoto in Japan and by German groups (Evenschor and Hauk, 1975a,b; Hauk and Sesemann, 1975; Dolle and Hauk, 1976, 1977; 1978; Peiter, 1976; Peiter and Lode, 1976; Lode and Peiter, 1977). There are two major ideas involved: ¬

1. As the stresses calculated from lattice strains represent values averaged over the penetration depth of the X-rays, it cannot be assumed a priori that the averaged stress components normal to the surface are zero, especially when the subgrain size is small, or when steep stress gradients are present. Localized stress fields of defects and stresses due to plastic anisotropy are considered as far as they contribute to the lattice strain or peak shift (Cullity, 1977). It has been shown by Peiter (1976) and by Dolle and Hauk (1976) that shear stresses normal to the surface can explain the experimental results found after tangent plastic deformation.
2. The classical equation (1) of X-ray stress analysis presumes that the X-ray elastic constants do not depend on φ and ψ and d is linear vs. $\sin^2\psi$. Occasionally large oscillations in d vs. $\sin^2\psi$ have been observed in textured materials (Fig. 2b). The current interpretations of this phenomenon are summarized in Table 1. Note that two of these utilize isotropic elastic theory and the third takes into account that in textured materials X-ray elastic

constants can depend on φ and ψ.

This general anisotropic theory of X-ray stress measurement which will be summarized here starts from the statistical theory of elasticity (Eshelby, 1957, 1959; Kröner, 1958, 1967; Kneer, 1965; Morris, 1970; and Wecker and Morris, 1978). It will be shown that the anisotropic equations reduce to the classical equations for X-ray stress analysis (Macherauch and Müller, 1961; Barrett and Massalski, 1966) when the X-ray elastic constants are isotropic.

2. Stress Measurement on Isotropic Materials

2.1 Isotropic X-ray Elastic Constants

It is necessary at the outset to realize the difference between the average X-ray and bulk elastic constants. The former refers to averaged single crystal constants of those crystallites diffracting - all with the same direction L_3 (see Fig. 1), whereas the latter are averaged over all crystals. Previous treatments by Voigt (1928) or Reuss (1929) (bulk elastic constants) and by Glocker (1938), Schiebold (1938) and Müller and Martin (1939) (X-ray elastic constants) neglect the interaction between a crystallite and its neighbours. Including the coupling (Eshelby, 1957, 1959) formulae exist only for the elastic constants of untextured materials (Bollenrath, Hauk and Müller, 1967), while bulk elastic constants can be calculated for quasi-isotropic and textured materials, see Table II. It is important to note that, in these treatments, the inhomogeneous surrounding grains of a crystallite are replaced by a quasihomogeneous environment having the macroscopic isotropic or anisotropic properties of the polycrystal. Therefore, for the X-ray measurement it is necessary that the beam irradiates an area large enough

so that a statistically relevant number of grains or subgrains are reflecting. For the evaluation of stresses, it is necessary to carry out measurements of interplanar spacings "d" for different directions $\underline{L}_3$, given by φ and ψ (see Fig. 1). As tensor components, e.g. the lattice deformation ϵ'_{33}, depend on the orientation of the coordinate system* to which they are related, for the calculation of stresses in the coordinate system of the sample $\underline{P}_i$ two things must be known: 1) The X-ray elastic constants in different laboratory systems $\underline{L}_i$ and 2) The relationship between stresses σ_{ij} in the system $\underline{P}_i$ and those in systems $\underline{L}_i$. If the material is quasiisotropic, X-ray elastic constants do not depend on $\underline{L}_i(\varphi\psi)$, but if it has texture, in general these constants vary with φ and ψ, as will be shown in Section 3.1.

In the laboratory systems $\underline{L}_i$ the relation between interplanar spacings "d" or lattice strains ϵ'_{33} and effective stresses σ'_{ij} can be written as:

$$\left\langle \frac{d_{\varphi\psi}-d_o}{d_o} \right\rangle = \langle \epsilon'_{33} \rangle = \langle (s'_{33ij} + t'_{33ij}) \cdot \sigma'_{ij} \rangle, \qquad (3)$$

where $d_{\varphi\psi}$ - interplanar spacing for direction $\underline{L}_3$

d_o - interplanar spacing of a stress-free sample

ϵ'_{33} - lattice strain normal to lattice planes (hkℓ) (in direction $\underline{L}_3$)

s'_{33ij} - single crystal compliances in system $\underline{L}_i$

t'_{33ij} - elastic interaction of a grain and its surrounding matrix ("elastic susceptibility")

σ'_{ij} - stress components in system $\underline{L}_i$

---

*Note that primed tensor components refer to the laboratory system $\underline{L}_i$, while unprimed refer to the sample system $\underline{P}_i$. Principal strains and stresses have single subscripts. Single crystal compliances $\tilde{s}_{ijk\ell}$ related to the principal axes of the (cubic) crystal are indicated by tilde.

The brackets in eqn. (3) indicate that an average is taken over the crystallites diffracting.

If the number of crystallites diffracting is large:

$$\langle \varepsilon'_{33} \rangle = \langle (s'_{33ij} + t'_{33ij}) \cdot \sigma'_{ij} \rangle = \langle (s'_{33ij} + t'_{33ij}) \rangle \langle \sigma'_{ij} \rangle \qquad (4)$$

where $\langle \sigma'_{ij} \rangle$ are the stresses averaged over the penetration depth and the equation

$$r'_{ij} \equiv \langle s'_{33ij} + t'_{33ij} \rangle$$

$$= \langle s'_{33ij} \rangle + \langle t'_{33ij} \rangle \qquad (5)$$

defines the X-ray elastic constants. The interaction term $\langle t'_{33ij} \rangle$ representing the coupling of a grain to the surrounding matrix depends on the single crystal constants and the texture.

For quaiisotropic materials the averages r'_{ij} in equation (5) do not depend on the orientation of the axes $\underline{L}_{i'}$ so that the prime can be omitted. Their relationships to the X-ray elastic constants $s_1(hk\ell)$ and $\frac{1}{2}\, s_2(hk\ell)$ defined by equation (1) are (Möller and Martin, 1939):

$$r_{11} = r_{22} \equiv s_1(hk\ell),$$

$$r_{33} \equiv s_1(hk\ell) + \tfrac{1}{2}\, s_2(hk\ell),$$

$$r_{12} \equiv r_{13} = r_{23} = 0. \qquad (6a,b,c)$$

If the interaction is neglected ($\langle t'_{33ij} \rangle = 0$), the Voigt averages taken over the single crystal stiffness coefficients (constant average strain) are obtained (Glocker, 1938; Schiebold, 1938; Möller and Martin, 1939):

$$s_1^V = \frac{\tilde{s}_o \cdot (\tilde{s}_{1111} + 2 \cdot \tilde{s}_{1122}) + 10 \cdot \tilde{s}_{1122} \cdot \tilde{s}_{1212}}{3 \cdot \tilde{s}_{1111} - 3\, \tilde{s}_{1122} + 4 \cdot \tilde{s}_{1212}}$$

$$\frac{1}{2G_V} = \tfrac{1}{2}\, s_2^V = \frac{10 \cdot \tilde{s}_{1212} \cdot (\tilde{s}_{1111} - \tilde{s}_{1122})}{3 \cdot \tilde{s}_{1111} - 3 \cdot \tilde{s}_{1122} + 4\, \tilde{s}_{1212}}\,, \qquad (7a,b)$$

with:

$$\tilde{s}_o = \tilde{s}_{1111} - \tilde{s}_{1122} - 2 \cdot \tilde{s}_{1212}. \qquad (8)$$

The Reuss averages, which are taken over the single crystal compliances (constant average stress), are (Glocker, 1938; Schiebold, 1938; Müller and Martin, 1939):

$$s_1^R(hk\ell) = \tilde{s}_{1122} + \tilde{s}_o \cdot \Gamma,$$

$$\tfrac{1}{2}\, s_2^R(hk\ell) = \tilde{s}_{1111} - \tilde{s}_{1122} - 3 \cdot \tilde{s}_o \cdot \Gamma, \qquad (9a,b)$$

with:

$$\Gamma = \frac{h^2k^2 + h^2\ell^2 + k^2\ell^2}{(h^2 + k^2 + \ell^2)^2}\,. \qquad (10)$$

Taking the crystal coupling into account (but <u>not</u> texture), Bollen rath, Hauk and Müller (1967) calculated X-ray elastic constants for quasi-isotropic polycrystals, which are in good agreement with experimental results (Macherauch and Wolfstieg, 1977), but it has been observed (Taira, Hayashi and Watase, 1968; Marion and Cohen, 1977; Dölle, Hauk, Kloth, Over, and Wichert, 1977) that X-ray elastic constants might vary with plastic deformation.

Based on the theoretical method of Eshelby (1957, 1959) and Kröner (1958, 1967) for a single phase cubic material the X-ray elastic constants can be calculated from (Bollen rath, Hauk and Müller, 1967):

$$s_1^K(hk\ell) = S_{3311} + t_{3311} + t_o \cdot \Gamma, \qquad (11a,b)$$

$$\tfrac{1}{2}\, s_2^K(hk\ell) = S_{3333} - S_{3311} + t_{3333} - t_{3311} - 3\, t_o \cdot \Gamma\,,$$

with

$$t_o = t_{3333} - t_{3311} - 2 \cdot t_{3131}. \qquad (12)$$

The bulk elastic constants S_{3333} and S_{3311}, which represent averages over s'_{33ij}, can be calculated from:

$$S_{3311} = \frac{1}{3}\left(\frac{1}{3K} - \frac{1}{2G}\right)$$

$$S_{3333} - S_{3311} = \frac{1}{2 \cdot G} \,. \qquad (13a,b)$$

According to Kröner's theory (1958, 1967) of quasiisotropic bulk elastic constants the compressibility K and the macroscopic shear modulus G can be calculated from single crystal compliances:

$$3K = \frac{1}{\tilde{s}_{1111} + 2 \cdot \tilde{s}_{1122}} \,,$$

$$G = G_V \cdot \left[1 - \frac{12}{125} \cdot \frac{ax^2}{1 - \frac{2}{25} \cdot a \cdot x - \frac{24}{625} \cdot a^2 x^2}\right] \qquad (14a,b)$$

with the Voigt-limit G_V from equation (7b), and:

$$a = \frac{3K + 6 \cdot G_V}{3K + 4 \cdot G_V} \,,$$

$$x = \frac{5 \cdot \tilde{s}_o}{3 \cdot \tilde{s}_{1111} - 3 \cdot \tilde{s}_{1122} + 4 \cdot \tilde{s}_{1212}} \,. \qquad (15a,b)$$

For a single-phase quasiisotropic material the tensor components t_{3333}, t_{3311} and t_{3131} can be calculated from:

$$t_{3333} = \frac{1}{3 \cdot G} \cdot \frac{2 \cdot G \cdot (\tilde{s}_{1111} - \tilde{s}_{1122}) - 1}{\frac{8G^2 + 9KG}{6G + 3K} \cdot (\tilde{s}_{1111} - \tilde{s}_{1122}) + 1}$$

$$t_{3311} = t_{3131} = -\tfrac{1}{2}\, t_{3333} \,. \qquad (16a,b)$$

A recent bibliography for the calculation of quasiisotropic X-ray elastic constants of multiphase or non-cubic materials was given by Dölle and Hauk (1977). The various isotropic X-ray elastic constants calculated for iron are shown in Fig. 3. For many practical purposes the medians (Neerfeld, 1942) from X-ray elastic constants in Voigt (equation 7) and Reuss-limit (equation 9) are sufficient. For the usual employed 211 and 310-reflections the difference between this median and Kröner values are less than 5%.

2.2 Lattice Strains in Isotropic Materials

The stresses related to the laboratory system $\underline{L}_i$ can be calculated from stress components σ_{ij} by

$$\sigma'_{ij} = \omega_{ik}\omega_{j\ell}\cdot\sigma_{k\ell} \tag{17}$$

where ω_{ij} are the direction cosines between both coordinate system $\underline{L}_i$ and $\underline{P}_i$. As shown in Fig. 1, $\underline{L}_2$ is in the sample surface and is parallel with the axis of ψ tilt. Therefore

$$\underline{\underline{\omega}} = \begin{pmatrix} \cos\varphi\cdot\cos\psi & \sin\varphi\cdot\cos\psi & -\sin\psi \\ -\sin\varphi & \cos\varphi & 0 \\ \cos\varphi\cdot\sin\psi & \sin\varphi\cdot\sin\psi & \cos\psi \end{pmatrix} \tag{18}$$

and the stresses σ'_{ij} result as

$$\begin{aligned}
\sigma'_{11} &= \sigma_{11}\cdot\cos^2\varphi\cdot\cos^2\psi + \sigma_{12}\sin^2\varphi\cdot\cos^2\psi - \sigma_{13}\cdot\cos\varphi\cdot\sin2\psi \\
&\quad + \sigma_{22}\cdot\sin^2\varphi\cdot\cos^2\psi - \sigma_{23}\sin\varphi\cdot\sin2\psi + \sigma_{33}\cdot\sin^2\psi \\
\sigma'_{12} &= \sigma'_{21} = -\tfrac{1}{2}\sigma_{11}\cdot\sin2\varphi\cdot\cos\psi + \sigma_{12}\cdot\cos2\varphi\cdot\cos\psi \\
&\quad + \sigma_{13}\cdot\sin\varphi\cdot\sin\psi + \tfrac{1}{2}\sigma_{22}\sin2\varphi\cdot\cos\psi - \sigma_{23}\cdot\cos\varphi\cdot\sin\psi \\
\sigma'_{13} &= \sigma'_{31} = \tfrac{1}{2}\sigma_{11}\cdot\cos^2\varphi\cdot\sin2\psi + \tfrac{1}{2}\sigma_{12}\cdot\sin2\varphi\cdot\sin2\psi + \sigma_{13}\cdot\cos\varphi\cdot\cos2\psi \\
&\quad + \tfrac{1}{2}\sigma_{22}\sin^2\varphi\cdot\sin2\psi + \sigma_{23}\sin\varphi\cdot\cos2\psi - \tfrac{1}{2}\sigma_{33}\sin2\psi
\end{aligned}$$

$$\sigma'_{22} = \sigma_{11}\cdot\sin^2\varphi - \sigma_{12}\cdot\sin 2\varphi + \sigma_{22}\cdot\cos^2\varphi$$

$$\sigma'_{23} = \sigma'_{32} = -\frac{1}{2}\sigma_{11}\cdot\sin 2\varphi\cdot\sin\psi + \sigma_{12}\cdot\cos 2\varphi\cdot\sin\psi - \sigma_{13}\cdot\sin\varphi\cdot\cos\psi + \frac{1}{2}\sigma_{22}\cdot\sin 2\varphi\cdot\sin\psi + \sigma_{23}\cdot\cos\varphi\cdot\cos\psi$$

$$\sigma'_{33} = \sigma_{11}\cdot\cos^2\varphi\cdot\sin^2\psi + \sigma_{12}\cdot\sin 2\varphi\cdot\sin^2\psi + \sigma_{13}\cdot\cos\varphi\cdot\sin 2\psi + \sigma_{22}\sin^2\varphi\cdot\sin^2\psi + \sigma_{23}\cdot\sin\varphi\cdot\sin 2\psi + \sigma_{33}\cdot\cos^2\psi \qquad (19)$$

According to equations (4), (5) and (19) the relationship between multiaxial stress-states and lattice deformation ε'_{33} or change in interplanar spacing "d" is (Dölle and Hauk, 1976):

$$\frac{d_{\varphi\psi} - d_o}{d_o} = \varepsilon'_{33} = \tfrac{1}{2}\, s_2(hk\ell)\cdot[\sigma_{11}\cdot\cos^2\varphi + \sigma_{12}\cdot\sin 2\varphi + \sigma_{22}\cdot\sin^2\varphi]\cdot\sin^2\psi + \tfrac{1}{2}\, s_2(hk\ell)\cdot\sigma_{33}\cdot\cos^2\psi + s_1(hk\ell)\cdot[\sigma_{11} + \sigma_{22} + \sigma_{33}] + \tfrac{1}{2}\, s_2(hk\ell)\cdot[\sigma_{13}\cdot\cos\varphi + \sigma_{23}\cdot\sin\varphi]\cdot\sin 2\psi \qquad (20)$$

where the stress components σ_{ij} are to be interpreted as average values over the penetration depth of the X-rays.

Consider the following four stress-tensors whose components are given relative to the sample system $\underline{P}_i$:

$$\begin{pmatrix} \sigma_1 & 0 & 0 \\ 0 & \sigma_2 & 0 \\ 0 & 0 & 0 \end{pmatrix} \quad \begin{pmatrix} \sigma_{11} & \sigma_{12} & 0 \\ \sigma_{12} & \sigma_{22} & 0 \\ 0 & 0 & 0 \end{pmatrix} \quad \begin{pmatrix} \sigma_1 & 0 & 0 \\ 0 & \sigma_2 & 0 \\ 0 & 0 & \sigma_3 \end{pmatrix} \quad \begin{pmatrix} \sigma_{11} & \sigma_{12} & \sigma_{13} \\ \sigma_{12} & \sigma_{22} & \sigma_{23} \\ \sigma_{13} & \sigma_{23} & \sigma_{33} \end{pmatrix} \qquad (21a\text{-}d)$$

While the tensors (21a,b) represent (residual or applied) stresses in free surfaces, the tensors (21c,d) may represent residual stress-states in the interior of a material or stress-states caused by multiaxial loading. It is obvious that for the tensors a and c the principal axes of the stress state coincide with the sample system P_i. The "classical" d-$\sin^2\psi$-law (1) (Macherauch and Müller, 1961) results, when (21a) is substituted into equation (20). For the tensors (21b,c) there are additional terms, but

d vs. $\sin^2\psi$ is still linear. For the most general stress state (21d) "d" is no longer linear vs. $\sin^2\psi$. The terms σ_{13} and σ_{23} in equation (20) have a $\sin 2\psi$ dependence. This results in different d vs. $\sin^2\psi$ relationships for $\psi > 0$ and $\psi < 0$ as illustrated in Fig. 2a. This effect has been termed "ψ-splitting" (Dölle and Hauk, 1977) and has actually been detected by Walburger (1973) in ground steel. In recent years these lattice strain distributions were found after grinding or milling (Faninger and Walburger, 1976; Wolfstieg and Macherauch, 1976; Macherauch and Wolfstieg, 1977; Dölle and Cohen, in press), or on the surfaces of wheels and wear (Christ and Krause, 1975; Krause and Jühe, 1976, 1977).

2.3 The Evaluation of the Stress Tensor for Isotropic Materials

The lattice strain for the direction $\underline{L}_3$ is (Evenschor and Hauk, 1975b):

$$\varepsilon'_{33} = \varepsilon_{11}\cdot\cos^2\varphi\cdot\sin^2\psi + \varepsilon_{12}\cdot\sin 2\varphi\cdot\sin^2\psi + \varepsilon_{13}\cdot\cos\varphi\cdot\sin 2\psi + \varepsilon_{22}\cdot\sin^2\varphi\cdot\sin^2\psi + \varepsilon_{23}\cdot\sin\varphi\cdot\sin 2\psi + \varepsilon_{33}\cdot\cos^2\psi \tag{22}$$

Introducing the average strain a_1 and the deviation, a_2, from this average strain ("ψ-splitting"):

$$a_1 = \tfrac{1}{2}[\varepsilon_{\varphi\psi+} + \varepsilon_{\varphi\psi-}] = \frac{d_{\varphi\psi+} + d_{\varphi\psi-}}{2d_o} - 1$$

$$= \varepsilon_{33} + [\varepsilon_{11}\cdot\cos^2\varphi + \varepsilon_{12}\cdot\sin 2\varphi + \varepsilon_{22}\cdot\sin^2\varphi - \varepsilon_{33}]\cdot\sin^2\psi \tag{23a}$$

$$a_2 = \tfrac{1}{2}[\varepsilon_{\varphi\psi+} - \varepsilon_{\varphi\psi-}] = \frac{d_{\varphi\psi+} - d_{\varphi\psi-}}{2d_o} \tag{23b}$$

$$= [\varepsilon_{13}\cdot\cos\varphi + \varepsilon_{23}\cdot\sin\varphi]\cdot\sin|2\psi|$$

Thus, ε_{33} can be determined from the intercept of a_1 vs. $\sin^2\psi$, if d_o is known. As a check on this result, note that this value is independent

of φ. The tensor components ε_{11} ε_{12} ε_{22} can be obtained from $(\frac{\partial a_1}{\partial \sin^2\psi})$. For $\varphi = 0$, $\varepsilon_{11} - \varepsilon_{33}$ is obtained, whereas for $\varphi = 90^\circ$, $\varepsilon_{22} - \varepsilon_{33}$ is evaluated. The tensor component ε_{12} can then be evaluated from $(\frac{\partial a_1}{\partial \sin^2\psi})$ at $\varphi = 45°$. From $(\frac{\partial a_2}{\partial \sin|2\psi|})$, ε_{13} results when $\varphi = 0$, and ε_{23} when $\varphi = 90^\circ$.

Taking the crystallographical anisotropy into account the stress components σ_{ij} can be calculated from

$$\sigma_{ij} = \frac{1}{\frac{1}{2}s_2(hk\ell)} \cdot \left[\varepsilon_{ij} - \delta_{ij} \cdot \frac{s_1(hk\ell)}{\frac{1}{2}s_2(hk\ell) + 3 \cdot s_1(hk\ell)} \cdot (\varepsilon_{11}+\varepsilon_{22}+\varepsilon_{33})\right] . \tag{24}$$

This method, developed by Dölle and Hauk (1976), can also be used when there is no ψ-splitting (which implies that $\sigma_{13} = \sigma_{23} = 0$). It may be a useful procedure to determine whether or not the surface stress condition $\sigma_{33} = 0$ is fulfilled.

An experimental example of this kind of study (Dölle and Cohen, in press) is discussed below: On a ground steel the ε-$\sin^2\psi$-curves shown in Fig. 4 were measured; the evaluation of stresses resulted the residual stress tensor

$$\begin{pmatrix} 390 & 14 & 63 \\ 14 & 306 & -1 \\ 63 & -1 & 92 \end{pmatrix} \qquad \text{(components in MPa)} \tag{25}$$

It is remarkable how well equation (20) with the stress tensor (25) substituted fit the data points. The principal axes of the stress tensor evaluated by principal axes transformation were tilted about the transverse direction of the sample $\underline{P}_2$ about 11 degrees.

3. Stress Measurement on Textured Materials

3.1 X-ray Elastic Constants of Textured Materials

For textured materials the X-ray elastic constants defined by equation (5), even for the same hkℓ reflection, depend on the direction $\varphi\psi$ of the measurement (Dölle and Hauk, 1978). Neglecting the interaction of crystallites ($t'_{33ij} = 0$) the anisotropic X-ray elastic constants will be calculated for a sharp texture in cold rolled α-iron, as an example of the procedures. Since the averages will be taken over single crystal compliances s'_{33ij}, the X-ray elastic constants will result in the Reuss limit. It will be assumed that the orientation distribution of the crystallites can be idealized by some combination of single crystal orientations with different volume fractions λ^a, and including a volume fraction λ^i of randomly oriented crystallites. A model similar to this has been employed by Alers and Liu (1966) for the calculation of anisotropic bulk elastic constants. Since the X-ray measurement is selective, it is necessary to modify their model in the following ways:

1. Since preferred orientations are assumed there are only a few directions $\Phi_i\Psi_i$ for which strong reflections are obtained.
2. Because the averages have to be taken over reflecting crystallites only, the anisotropic X-ray elastic constants are obtained only for these directions $\Phi_i\Psi_i$. Therefore, the orientation distribution functions, which are constant for quasiisotropic materials, can be represented by δ-function being zero unless $\varphi = \Phi_i$ and $\Psi = \Psi_i$.

Using the isotropic X-ray elastic constants $r_{ij}(hk\ell)$, equation (6), the anisotropic X-ray elastic constants R'_{ij} of such an idealized polycrystal

can be calculated by assuming (Dölle, Hauk, and Zegers, 1978):

$$R'_{ij}(hk\ell\Phi\Psi) = \frac{\lambda^i \cdot r_{ij}(hk\ell) + \lambda^a \cdot \langle s'_{33ij} \rangle^a}{\lambda^i + \lambda^a}, \qquad (26)$$

where anisotropic averages $\langle s'_{33ij} \rangle^a$ have to be taken over the preferred orientations. If the crystallites with random orientations are neglected, $\lambda^i = 0$, and there is no superposition of the different preferred orientations for a given direction $\Phi_i\Psi_i$, R'_{ij} does not depend on the volume fractions λ^a. In this case, R'_{ij} is equal to the single crystal compliances s'_{33ij} referred to the laboratory-system $\underline{L}_i(\Phi_i\Psi_i)$. If there are no preferred orientations, $\lambda^a = 0$, the isotropic X-ray elastic constants in the Reuss-limit (equation 9) result from equation (26). It is evident that by taking the weighted averages (26) , the texture of the material is taken into account in a quantitative way. However, these averages and the isotropic and anisotropic limits discussed above do not consider the interaction of crystallites. Additionally, real orientation distributions of crystallites are much more complicated than the assumed ones, but it will be shown that this anisotropic theory of X-ray measurement can explain many of the observed phenomena associated with textured materials, at least qualitatively and in some cases quantitatively.

In what follows, the directions $\Phi_i\Psi_i$ of strong reflections and the anisotropic averages $\langle s'_{33ij} \rangle^a$ related to the laboratory-systems $\underline{L}_i(\Phi_i\Psi_i)$ will be calculated for the following preferred orientations of α-iron:

(211) $[01\bar{1}]$ or $[0\bar{1}1]$,

(111) $[\bar{2}11]$ or $[2\bar{1}\bar{1}]$,

(100) $[011]$. (27)

A (211) $[01\bar{1}]$ orientation implies that the (211) plane of a crystallite is parallel to the rolling plane and the $[01\bar{1}]$ direction is parallel to the rolling direction. Therefore, the unit vectors coinciding with the rolling (RD), transverse (TD) and normal (ND) direction are:

$$\text{RD:}\quad \underline{B}_1 = \frac{1}{\sqrt{2}}\,[01\bar{1}],$$

$$\text{ND:}\quad \underline{B}_3 = \frac{1}{\sqrt{6}}\,[211],$$

$$\text{TD:}\quad \underline{B}_2 = \underline{B}_3 \times \underline{B}_1 = \frac{1}{\sqrt{3}}\,[\bar{1}11], \tag{28}$$

where components of the unit vectors $\underline{B}_i$ are related to the crystal axes $\underline{A}_j$. The direction cosines β_{ij} describing the orientation of a crystallite with respect to the coordinate system $\underline{B}_i$ are:

$$\beta_{ij} = (\underline{B}_j \cdot \underline{A}_j) = \begin{pmatrix} 0 & \frac{1}{\sqrt{2}} & \frac{\bar{1}}{\sqrt{2}} \\ \frac{\bar{1}}{\sqrt{3}} & \frac{1}{\sqrt{3}} & \frac{1}{\sqrt{3}} \\ \frac{2}{\sqrt{6}} & \frac{1}{\sqrt{6}} & \frac{1}{\sqrt{6}} \end{pmatrix} \tag{29}$$

If a sample is cut from a rolled sheet in an arbitrary way, the orientation of a crystallite with respect to the coordinate system $\underline{P}_i$ of the sample is:

$$\pi_{ij} = (\underline{P}_j \cdot \underline{A}_j) = \eta_{ik} \cdot \beta_{kj}. \tag{30}$$

The matrix elements π_{ij} $(j = 1,3)$ are the components of the unit-vectors $\underline{P}_i$ with respect to the crystal axes $\underline{A}_j$ and η_{ik} are the direction cosines between the coordinate systems $\underline{P}_i$ and $\underline{B}_k$.

$$\eta_{ik} = (\underline{P}_i \cdot \underline{B}_k). \tag{31}$$

If samples are cut with the rolling planes in their surfaces ($\underline{P}_3 = \underline{B}_3$), $\underline{\underline{\eta}}$ has the form:

$$\underline{\underline{\eta}} = \begin{pmatrix} \cos\zeta & \sin\zeta & 0 \\ -\sin\zeta & \cos\zeta & 0 \\ 0 & 0 & 1 \end{pmatrix} \tag{32}$$

where ζ is the angle from the rolling direction $\underline{B}_1$ to the longitudinal direction of the sample, $\underline{P}_1$. For a sample with the rolling direction $\underline{B}_1$ as $\underline{P}_1$ ($\zeta = 0$), $\underline{\underline{\eta}}$ is the unit-matrix δ_{ij}.

The directions $\Phi_i\Psi_i$ of a strong reflection from the {hkℓ} planes chosen for the measurement of interplanar spacings are called the poles of hkℓ reflections. These angles can be calculated for each of the assumed preferred orientations specified in terms of $\underline{P}_i$ as follows:

$$q_1 = (\underline{P}_1 \cdot \underline{E}_i) \text{ and } q_2 = (\underline{P}_2 \cdot \underline{E}_i) \tag{33a,b}$$

$$\tan\Phi_i = \frac{q_2}{q_1} \text{ and } \sin^2\Psi_i = q_1^2 + q_2^2 \tag{34a,b}$$

The $\underline{E}_i$ are the unit-vectors in the crystal's axial system belonging to the hkℓ reflection and all planes in the form must be considered. The reflections most commonly employed in stress measurements on steels are the 211 and 310. The poles of these planes within the usual measuring range $\sin^2\Psi \leq 0.5$ are shown in Fig. 5. The numerical values of Φ_i and Ψ_i and the specific planes reflecting are listed in Table III.

For the calculation of transformed single crystal compliances s'_{33ij}, related to the system $\underline{L}_i$ (see Fig. 1), it is necessary to evaluate the components of $\underline{L}_i$ in terms of the crystal coordinates $\underline{A}_j$. The vector $\underline{L}_3$ is identical with the particular unit-vector $\underline{E}_i$, whose orientation with respect to the sample system $\underline{P}_i$ is given by Φ_i and Ψ_i. Its components

$\gamma_{31}\gamma_{32}\gamma_{33}$ expressed in crystal coordinates are:

$$\gamma_{31} = \frac{h}{\sqrt{h^2 + k^2 + \ell^2}}; \quad \gamma_{32} = \frac{k}{\sqrt{h^2 + k^2 + \ell^2}}; \quad \gamma_{33} = \frac{\ell}{\sqrt{h^2 + k^2 + \ell^2}} \tag{35a,b,c}$$

The vector components $\gamma_{21}\gamma_{22}\gamma_{23}$ of the unit vector $\underline{L}_2$ can be evaluated from the rotation around $\underline{P}_3$, keeping in mind that $\underline{L}_2$ is in the sample's surface (Fig. 1):

$$\underline{L}_2 = \begin{pmatrix} \gamma_{21} \\ \gamma_{22} \\ \gamma_{23} \end{pmatrix} = \underline{\underline{\omega}}_i \cdot \underline{P}_2 = \begin{pmatrix} \cos\Phi_i & \sin\Phi_i & 0 \\ -\sin\Phi_i & \cos\Phi_i & 0 \\ 0 & 0 & 1 \end{pmatrix} \cdot \begin{pmatrix} \pi_{21} \\ \pi_{22} \\ \pi_{23} \end{pmatrix}, \tag{36}$$

The unit vector $\underline{L}_1$ can be calculated from:

$$\underline{L}_1 = \begin{pmatrix} \gamma_{11} \\ \gamma_{12} \\ \gamma_{13} \end{pmatrix} = \underline{L}_2 \times \underline{L}_3. \tag{37}$$

The single crystal compliances in the laboratory system $\underline{L}_i$ are obtained from the usual equations for the transformation of tensor components:

$$s'_{33ij} = \gamma_{3m}\gamma_{3n}\cdot\gamma_{io}\cdot\gamma_{jp}\cdot\tilde{s}_{mnop} \tag{38}$$

With $\tilde{s}_o$ defined in equation (8) the transformed tensor component s'_{33ij} result as:

$$\begin{aligned}
s'_{3311} &= \tilde{s}_{1122} + \tilde{s}_0\cdot\gamma_{1k}^2\gamma_{3k}^2, \\
s'_{3322} &= \tilde{s}_{1122} + \tilde{s}_0\cdot\gamma_{2k}^2\gamma_{3k}^2, \\
s'_{3333} &= \tilde{s}_{1122} + 2\tilde{s}_{1212} + s_0\gamma_{3k}^4, \\
s'_{3312} &= \tilde{s}_0\gamma_{1k}\gamma_{2k}\gamma_{3k}^2, \\
s'_{3313} &= \tilde{s}_0\gamma_{1k}\gamma_{3k}^3, \\
s'_{3323} &= \tilde{s}_0\gamma_{2k}\gamma_{3k}^3.
\end{aligned} \tag{39a-f}$$

As preferred orientations have been assumed the term $\langle s'_{33ij} \rangle^a$ in equation (26) is given by (39). Also, as

$$(\underline{L}_i \underline{L}_j) = \gamma_{ik} \cdot \gamma_{jk} = \delta_{ij} \tag{40}$$

for the h00 and hhh-reflections quasi-isotropic X-ray elastic constants result from the anisotropic theory, which are identical with the results from equation (9). For these reflections, by substituting (40) in (39) it can be shown that s'_{3312}, s'_{3313} and s'_{3323} are zero and therefore, the same conditions as for quasi-isotropic materials (see Section 2) can be expected; these reflections are not affected by texture.

Anisotropic X-ray elastic constants for the poles of the 211 and 310-reflections have been calculated for volume fraction λ^i and λ^a corresponding to the intensity distributions published in the literature (Shiraiwa and Sakamoto, 1970; Hauk, Herlach and Sesemann, 1975). The volume fractions assumed and the calculated anisotropic X-ray elastic constants R'_{ij} are listed in Table III.

Anisotropic X-ray elastic constants recently evaluated by Dölle, Hauk and Zegers (1978) for the 211-reflection of cold rolled steels are shown in Fig. 6. The experimental results for $\psi_i = 0$ and various angles ζ (see Fig. 5) lie between the isotropic limit calculated from equation (9a) and the anisotropic limit for the case of the $(211)[0\bar{1}1]$ or $[0\bar{1}\bar{1}]$ orientation, which furnishes the pole for $\psi_i = 0$, see Fig. 5. As the crystallographic direction changes with the cut-out direction, the anisotropic limit depends on the angle ζ. Although additional experiments are necessary, it is obvious that with increasing degree of reduction the experimental values approach the anisotropic limit. However, this limit cannot be reached with a real material because it represents the elastic behavior of a free (uncoupled) single crystal.

3.2 Lattice Strains in Textured Materials

For anisotropic materials, lattice strains vs. $\sin^2\psi$ can be calculated from (Dölle and Hauk, 1978):

$$\epsilon'_{33} = \frac{d_{\varphi\psi} - d_o}{d_o} = R'_{ij} \cdot \sigma'_{ij}. \tag{41}$$

In general, R'_{12}, R'_{13} and R'_{23} are different from zero in textured materials, see Table III. Thus, shear stresses σ'_{ij} might also cause normal strains ϵ'_{33} normal to the lattice plane. Using the results from equations (19) the relationship between lattice strains ϵ'_{33} and stresses σ_{ij} related to the sample system $\underline{P}_i$ is (Dölle and Hauk, in press):

$$\begin{aligned}
\frac{d_{\varphi\psi} - d_o}{d_o} = \epsilon'_{33} = {} & [R'_{11}\cdot\cos^2\varphi\cdot\cos^2\psi + R'_{22}\cdot\sin^2\varphi + R'_{33}\cdot\cos^2\varphi\cdot\sin^2\psi \\
& - R'_{12}\cdot\sin2\varphi\cdot\cos\psi + R'_{13}\cdot\cos^2\varphi\cdot\sin2\psi - \\
& - R'_{23}\cdot\sin2\varphi\cdot\sin\psi]\cdot\sigma_{11} \\
& + [R'_{11}\cdot\sin^2\varphi\cdot\cos^2\psi + R'_{22}\cdot\cos^2\varphi + R'_{33}\cdot\sin^2\varphi\cdot\sin^2\psi \\
& + R'_{12}\cdot\sin2\varphi\cdot\cos\psi + R'_{13}\cdot\sin^2\varphi\cdot\sin2\psi + R'_{23}\cdot\sin2\varphi\cdot\sin\psi]\cdot\sigma_{22} \\
& + [R'_{11}\cdot\sin2\varphi\cdot\cos^2\psi - R'_{22}\cdot\sin2\varphi + R'_{33}\cdot\sin2\varphi\cdot\sin^2\psi \\
& + 2\cdot R'_{12}\cos2\varphi\cdot\cos\psi + R'_{13}\cdot\sin2\varphi\cdot\sin2\psi + 2\cdot R'_{23}\cdot\cos2\varphi\cdot\sin\psi]\cdot\sigma_{12} \\
& + [R'_{11}\cdot\sin^2\psi + R'_{33}\cdot\cos^2\psi - R'_{13}\cdot\sin2\psi]\cdot\sigma_{33} \\
& + [-R'_{11}\cdot\cos\varphi\cdot\sin2\psi + R'_{33}\cdot\cos\varphi\cdot\sin2\psi + 2R'_{12}\cdot\sin\varphi\cdot\sin\psi \\
& + 2\cdot R'_{13}\cdot\cos\varphi\cdot\cos2\psi - 2\cdot R'_{23}\cdot\sin\varphi\cdot\cos\psi]\cdot\sigma_{13} \\
& + [-R'_{11}\cdot\sin\varphi\cdot\sin2\psi + R'_{33}\cdot\sin\varphi\cdot\sin2\psi - 2\cdot R'_{12}\cdot\cos\varphi\cdot\sin\psi \\
& + 2\cdot R'_{13}\cdot\sin\varphi\cdot\cos2\psi + 2R'_{23}\cdot\cos\varphi\cdot\cos\psi]\cdot\sigma_{23} \\
= {} & F_{ij}(\varphi\psi R'_{ij}) \cdot \sigma_{ij}.
\end{aligned} \tag{42}$$

As opposed to R'_{ij} the terms F_{ij} in the above equation are not tensor components. Their numerical values for the poles of the 211 and 310-reflections are also listed in Table III. When isotropic X-ray elastic constants (equation 6) are substituted into (42) , equation (20) results and if the tensor (21a) is employed, the $\sin^2\psi$ law (1) is obtained.

Some characteristic plots of lattice strain vs. $\sin^2\psi$ will be presented for the 211-reflection. For different samples cut at various angles ζ for the same stress σ_{11} = 100 MPa different curves of ϵ vs. $\sin^2\psi$ result, as shown in Fig. 7. Strong oscillations which have been observed by many authors (Bollen rath, Hauk and Weidemann, 1967; Shiraiwa and Sakamoto, 1970; Marion and Cohen, 1975; Hauk, Herlach and Seseman, 1975; Dölle, Hauk and Zegers, 1978), only occur for the rolling direction, $\zeta = 0$. The reason for this effect is a change in the sign of R'_{13} for the three poles at $\psi_i = 0$, 13.5° and 33.6°, see Table III. For that reason, an earlier calculation (Evenschor and Hauk, 1975a) of lattice strain distributions under the presumption $R'_{13} = 0$ could not yield the oscillations observed in experimental studies. A further examination of Fig. 6 and Table III, especially of the X-ray constants for $\psi_i = 0$, shows that R'_{11} and R'_{22} (connected with σ_{11} and σ_{22}) depend on which crystallographic direction is parallel to each $\underline{L}_2(\Phi_i, \psi_i = 0)$. The change of the elastic constants R'_{11} and R'_{22} with the orientation $\Phi\psi$ is about three times smaller than the variation in R'_{13}. The amount of oscillation in d vs. $\sin^2\psi$ for a coarse grained material results from the variation of all elastic constants R'_{ij}.

However, oscillations due to grain statistics are only likely in recrystallized material, but not in cold worked materials. It is obvious that erroneous stresses might be obtained if any two tilt method is employed for the measurement of stresses in textured materials.

Comparing the upper diagrams of Fig. 9 (isotropic case) with the lower diagrams (measurements for the 3 poles in the roling direction) it is clear that transverse stresses σ_{22} may cause additional oscillations in ϵ-$\sin^2\psi$-plots. Whereas $s_1(hk\ell)$, connected with σ_{22} according to equation (20) does not depend on ψ, R'_{22} or F_{22} (see Table III), changes during the ψ-tilt and this causes oscillations. It is obvious that, when shear stresses σ_{13} or σ_{23} are present, a ψ-splitting in the nonlinear d-$\sin^2\psi$ plots occur.

The lattice strains and the oscillations in d-$\sin^2\psi$- curves calculated by the equations presented here will be larger than those in real textured aggregates, because the effects of crystal coupling or plastic deformation have been neglected. Additionally, if the rolling deformation is not too great, the influence of the fraction of crystallites with random orientations in equation (26) will be large. Since for h00- and hhh-reflections the X-ray elastic constants do not depend on the direction φ ψ of the measurement, the same ϵ-$\sin^2\psi$ distribution as in isotropic materials appears. However, the calculations have been carried out neglecting the interaction terms t'_{33ij} (5). Therefore oscillations might be observed with these reflections and tests are underway (Dölle and Cohen, to be published) to see if these reflections are more useful for stress measurements than the currently popular 211 and 310 reflections. In fact on examining Fig. 5 it is clear that the 310 reflection will exhibit less oscillation due to elastic anisotropy in iron in

both the rolling and transverse directions.

3.3 Evaluation of Stresses in Textured Materials

Three methods have been described in the literature: The method of texture independent directions by Hauk and Sesemann (1976), the Shiraiwa-Sakamoto method (1970, 1972) and the method of Marion and Cohen (1974), see Table I. All methods presume that the directions of principal stresses are known. Recently, a method for the evaluation of multiaxial stress states (21d) in textured materials, basing on anisotropic theory of elasticity, has been developed. This new method will be discussed here, also (Dölle and Hauk, in press).

The method of texture independent directions have been developed to evaluate uniaxial residual or applied stresses in textured materials. For particular directions and reflections there are ψ-angles for which the isotropic lattice strain (equation 20) is equal to the lattice strain in textured materials (equation 42). These ψ-directions are the intersection points ψ^{**} in Fig. 7a. Two intersections are required and this occurs only in the rolling direction. The stresses can be calculated from the "quasi-isotropic" strains by using isotropic X-ray elastic constants, as in Chapter 2.1. For uniaxial stress conditions good agreement is obtained between stresses evaluated in this manner and the applied load (Hauk, Herlach and Sesemann, 1975). However, for multiaxial stress-states this method cannot be employed because the texture independent directions depend on the magnitude of the stress-components as well as on X-ray elastic constants.

Shiraiwa and Sakamoto (1970) evaluated residual stresses in textured materials, by employing single crystal compliances $\tilde{s}_{ijkl}$ for strains measured at the poles in a pole figure,

see Fig. 5. The equation used was:

$$\epsilon'_{33} = \{2 \cdot s_{1212} \cdot \sin^2\psi_i + \tilde{s}_o \cdot \gamma_{3k}^2 \chi_{k1}^2 + \tilde{s}_{1122}\} \cdot \sigma_1 + \{\tilde{s}_o \cdot \gamma_{3k}^2 \chi_{k2}^2 + \tilde{s}_{1122}\} \cdot \sigma_2 \tag{43}$$

where γ_{3k} has been explained in equation (35) and χ_{ki} are the direction cosines between the crystallographic axes (k) and the principal axes (i) of the stress-tensor (21a). This model of uncoupled crystallites (Reuss, 1929; Möller and Martin, 1939) has been put in a more general form by Dölle and Hauk (1978) and has been described in the previous section 3.1 and 3.2.

The method of Marion and Cohen (1975) starts from considerations of Greenenough (1951) and of Bollenrath, Hauk and Weidemann (1967). While the first author considered microstresses in quasi-isotropic materials, the latter correlated the lattice strain, and especially the oscillations in d vs. $\sin^2\psi$, with the deformation texture. The equation used for the evaluation of "macro-stress" σ_1 parallel to the rolling direction is (Weidemann, 1966):

$$d_{\varphi=0,\psi} = \tfrac{1}{2}s_2(hk\ell) \cdot d_o \cdot \sigma_1 \cdot \sin^2\psi + d_B + (d_{max} - d_B) \cdot f(0,\psi) \tag{44}$$

where the first term describes strains due to macrostresses (linear with $\sin^2\psi$) and the last one oscillations due to microstresses. d_B is the interplanar spacing in dislocation poor regions, d_{max} the interplanar spacing for the direction of strongest reflection and $f(0,\psi)$ the intensity distribution for the rolling direction. The function $f(0,\psi)$ is normalized by setting $f(0,\psi) = 1$ for the maximum integrated intensity. The major deficiency

involved in this method is that isotropic X-ray elastic constants are used. The theory described in the previous section clearly shows that oscillations may also occur from homogeneous stresses in textured material due to elastic anisotropy.

Starting from equation (42) Dölle and Hauk (in press) recently presented a method for the evaluation of multiaxial stress-states (21d) in textured materials. The authors suggested carrying out measurements (intensity and peak location) for the directions $\Phi_i\Psi_i$ of a pole figure, see Figure 5. When the interplanar spacing d_o of the stress-free state is known, stresses can be evaluated from strains by a least square fit to equation (42) using experimental values of X-ray elastic constants or these calculated according to equation (26) (see also Table III). If there is evidence for a surface stress-state (21ab), the last three terms in equation (42) can be omitted and a least-square fit can be computed for the variables $\sigma_{11}\sigma_{12}\sigma_{22}$ only. Unfortunately, this method is not simple enough to be employed in practical situations. Therefore, as an alternative, the measurement (Dölle and Cohen, to be published) can be performed with the 310, h00- or hhh-reflections. Since no (or only small) oscillations should occur according to this approach, the methods of Chapter 2.3 or the classical methods can be used to evaluate the stresses.

Definitive experiments to decide between the interpretation based on microstresses or the one based on macrostresses and texture are surely needed.

4. The Influence of Steep Stress Gradients

The influence of stress gradients on a stress measurement with X-rays was first discussed by Osswald (1948) and later by Macherauch (1956); Kelly, Short and Evans (1971); Shiraiwa and Sakamoto (1972); Lei and Scardina (1976). In general, corrections due to the penetration depth τ of X-rays and the removal of surface layers (Kelly et al., 1971; Lei and Scardina, 1976) are necessary. It is well known that the average stress being evaluated by X-rays deviates from the stress in the surface when gradients are bigger than 2MPa μm^{-1}. However, for ground or shot peened surfaces of steels, steep gradients sometimes occur which can be bigger than this limit by a factor of 10 or more (Lessels and Brodrick, 1956; Iwanaga, Namikawa and Aoyama, 1972; Shiraiwa and Sakamoto, 1972; Schreiber, 1976).

Additionally, the influence of such stress-gradients on the linearity of d vs. $\sin^2\psi$ has been studied. While Shiraiwa and Sakamoto (1972) and Dölle (1978) calculated only small non-linearities for the stress-tensors in equation (21a) with gradients in σ_{11} and σ_{22}, Peiter and Lode (1976) argued, that multiaxial stress-states (tensor 21d) and steep gradients are the reasons for oscillations in d vs. $\sin^2\psi$ curves, see Table I. However, the theory of Peiter and Lode (1976) is defective because the absorption of X-rays was taken into account in an unrealistic way, and, indeed, there is no experimental evidence for this explanation, because oscillations usually persist even after the near surface layers are removed (Dölle, Hauk and Zegers, 1978; Quesnel, Meshii and Cohen, 1979).

In the following, a theoretical approach to the problem of near surface stress gradients will be presented, which can be employed for isotropic as well as for textured materials. For the calculation it will be assumed

that the interplanar spacing d_o of the stress-free state and the X-ray elastic constants are not altered by a free surface (Stickforth, 1966), where $z = 0$. Actually, slow variations of both parameters will not affect the results. In the surface, only the stress tensor (21b) is possible, while in the interior of the sample the general stress state (21d) can occur. Thus, not only gradients in $\sigma_{11}\sigma_{12}$ and σ_{22} have to be taken into account, but also for the other stress components. Note, that the effect of ψ-splitting discussed in Section 2.2, is impossible unless gradients with respect to z in σ_{13} or σ_{23} are present, because these components must vanish at the surface. It will also be assumed that the stress components σ_{ij} depend only on z, and that local strains $\varepsilon_{33}(\varphi,\psi,z)$ are caused by local stresses $\sigma_{ij}(z)$. The intensity (I) reflected by a unit-volume dV in the depth z can be written (Macherauch, 1956; Cullity, 1956):

$$dI \sim \exp\{-\mu\ell\}\cdot dV, \tag{45}$$

where ℓ is the path length of the X-ray beam within the sample and μ is the linear absorption coefficient. The path length depends on ψ and the Bragg-angle θ. For a Ω-goniometer the ψ-tilt occurs about the 2θ axes, which is perpendicular to the diffractometer plane. Therefore,

$$\ell = \frac{2\sin\theta\cdot\cos\psi}{\sin^2\theta-\sin^2\psi}\cdot z \quad . \tag{46a}$$

In recent years, in Europe the ψ-goniometer (Macherauch and Wolfstieg, 1977) has become popular, for which the ψ-tilt is around an axis, perpendicular to the 2θ-axis and parallel to the goniometer plane . For this geometry:

$$\ell = \frac{2}{\sin\theta\cdot\cos\psi}\cdot z. \tag{46b}$$

Defining the actual penetration depth of X-rays by:

$$\exp\{-\mu\ell\} = 1/e \quad \text{for } z = \tau, \tag{47}$$

the penetration depth becomes (Wolfstieg, 1976):

$$\tau_\Omega = \frac{\sin^2\theta - \sin^2\psi}{2\mu \cdot \sin\theta \cdot \cos\psi}, \tag{48a}$$

$$\tau_\psi = \frac{\sin\theta \cdot \cos\psi}{2\mu}, \tag{48b}$$

and the intensity can be rewritten as:

$$dI \sim \exp\{-\frac{z}{\tau}\}dV. \tag{49}$$

Therefore, the information included in a strain average over a depth z $\langle \varepsilon'_{33}(\varphi,\psi)\rangle$ is:

$$\langle \varepsilon'_{33}(\varphi,\psi)\rangle = \frac{\int_0^D \varepsilon'_{33}(\varphi,\psi,z)\cdot\exp\{-\frac{z}{\tau}\}dz}{\int_0^D \exp\{-\frac{z}{\tau}\}dz}, \tag{50}$$

where D is the thickness of the sample. For isotropic materials ε'_{33} from equation (20) has to be substituted in equation (50). For $\varphi = 0$:

$$\langle \varepsilon'_{33}(\varphi,\psi)\rangle = \tfrac{1}{2}\, s_2(hk\ell)\cdot[\langle\sigma_{11}\rangle\cdot\sin^2\psi + \langle\sigma_{13}\rangle\cdot\sin 2\psi + \langle\sigma_{33}\rangle\cdot\cos^2\psi] + s_1(hk\ell)\cdot[\langle\sigma_{11}\rangle + \langle\sigma_{22}\rangle + \langle\sigma_{33}\rangle], \tag{51}$$

with:

$$\langle\sigma_{ij}\rangle = \frac{\int_0^D \sigma_{ij}(z)\cdot\exp\{-\frac{z}{\tau}\}dz}{\int_0^D \exp\{-\frac{z}{\tau}\}dz},$$

$$\approx \sigma_{ij}(z=0) + \int_0^D \exp\{-\frac{z}{\tau}\}\cdot g_{ij}(z)dz, \tag{52}$$

where $g_{ij}(z)$ are the stress gradients with respect to the depth z:

$$g_{ij}(z) = \frac{d}{dz}\sigma_{ij}(z). \qquad (53)$$

Thus, the resulting d vs. $\sin^2\psi$ will be determined by the stresses in the surface ($z=0$), the stress gradients near the surface and the penetration depth $\tau(\psi,\theta)$. Typical d vs. $\sin^2\psi$ plots are shown in Fig. 9. Only when steep gradients are present the second term in equation (52) will contribute appreciably to the average strain measured. The non-linearities in d-$\sin^2\psi$ plots caused by gradients are generally small.

The theory presented is equivalent to the considerations of Shiraiwa and Sakamoto (1972) if the stress-tensor (Equation 21a) is substituted into equation (50). Moreover, when equation (42) is substituted into (50), the influence of stress gradients on d vs. $\sin^2\psi$ for textured materials can be found.

5. Conclusions

Recommendations for the practical application of X-ray stress measurement have been developed by American, Japanese and German groups. Unfortunately, these recommendations do not include the problem of nonlinear d vs. $\sin^2\psi$ distributions detected in recent years. Thus, the information presented here should be considered, when a stress evaluation is performed on heavily cold-worked materials (Dölle and Hauk, 1977, James and Cohen, in press).

In general, the influence of gradients, shear stresses and texture may be present at the same time but usually only one influence is dominant. If the two tilt method is employed nonlinear d vs. $\sin^2\psi$ can lead to erroneous results. Therefore, this approach should be employed only when the deformation history is known and a linear d-$\sin^2\psi$-dependence can be expected or has been verified in the laboratory.

In order to recognize ψ-splitting caused by machining, measurements are necessary for positive and negative ψ-directions or with ψ positive and at φ and $\varphi + 180°$. Since misalignments of the goniometer can cause an apparent ψ-splitting, this source of errors must be carefully eliminated in alignment, and checked by examining d vs. $\sin^2\psi$ for $\pm\psi$.

If the material has a strong texture, d-$\sin^2\psi$-distributions for the same direction on the specimen depend strongly on the hkℓ planes. It may be possible to circumvent these oscillations in d vs. $\sin^2\psi$ by employing h00 or hhh-reflections. Alternatively, quasi-isotropic directions or anisotropic X-ray elastic constants can be employed. With steels there is less effect with the 310 reflection than the 211. Stress gradients cause additional small nonlinearities. As the effects of shear-stresses and texture superimpose on the small effects due to gradients, the stress distribution should be evaluated by etching.

Acknowledgements

First of all, the author wishes to express his gratitude to Prof. V. Hauk, T.H. Aachen, Germany, with whom many of the basic ideas in this paper have been developed. Further he likes to thank Prof. J. B. Cohen for his assistance in preparing this manuscript and for many valuable comments. He also wishes to express his appreciation for support during his visit to Northwestern University, by the U.S. Office of Naval Research and Council for International Exchange of Scholars (Fulbright grant).

References

Alers, G. A. & Liu, Y. C. (1966). Trans. TMS-AIME 236, 482-489.

Barrett, C. S. & Massalski, T. B. (1966). Structure of Metals, 3rd ed., p. 466ff. New York: McGraw-Hill.

Bollenrath, F., Hauk, V. & Müller, E. H. (1967). Z. Metallkde. 58, 76-82.

Bollenrath, F., Hauk, V. & Weidemann, W. (1967). Z. Metallkde. 58, 643-649.

Christ, E. & Krause, H. (1975). Z. Metallkde. 66, 615-618.

Cullity, B. D. (1956). Elements of X-ray Diffraction, pp. 188-189. Reading, Mass.: Addison-Wesley.

Cullity, B. D. (1963). Trans. TMS-AIME 227, 356-358.

Dölle, H. & Hauk, V. (1976). Härterei-Techn. Mitt. 31, 165-168.

Dölle, H. & Hauk, V. (1977). Z. Metallkde. 68, 725-728.

Dölle, H., Hauk, V., Kloth, H., Over, H. & Wichert, W. (1977). Arch. Eisenhüttenwesen. 48, 601-605.

Dölle, H. (1978). Einfluss von Textur, Mehrachsigkeit des Spannungszustandes und Temperatur auf die Röntgenographische Spannungsermittlung von Stählen. Ph.D. Thesis, Technische Hochschule, Aachen, Germany.

Dölle, H. & Hauk, V. (1978). Z. Metallkde. 69, 410-417..

Dölle, H., Hauk, V. & Zegers, H. (1978). Z. Metallkde. 69, 766-772.

Dölle, H. & Hauk, V. (in press). Z. Metallkde.

Dölle, H. & Cohen, J. B. To be published.

Eshelby, J. D. (1957). Proc. Roy. Soc. London, Sec. A. 241, 376-396.

Eshelby, J. D. (1959). Proc. Roy. Soc. London, Sec. A. 252, 561-569.

Evenschor, P. D. & Hauk, V. (1975). Z. Metallkde. 66, 164-166.

Evenschor, P. D. & Hauk, V. (1975). Z. Metallkde. 66, 167-168.

Fachausschuss Spannungsmesstechnik. (1976). Spannungsermittlung mit Röntgentrahlung. In Härterei-Tech. Mitt. 31, #1 & 2. Munich: Hanser-Verlag.

Faninger, G. (1966). Acta Physica Austriaca 24, 245-270.

Faninger, G. & Walburger, H. (1976). Härterei-Techn. Mitt. 31, 79-82.

Glocker, R. (1938). Z. f. Techn. Physik 19, 289-293.

Greenenough, G. B. (1951). J. Iron a. Steel Inst. 169, 235-241.

Hauk, V., Herlach, D. & Sesemann, H. (1975). Z. Metallkde. 66, 734-737.

Hauk, V., & Sesemann, H. (1976). Z. Metallkde. 67, 646-650.

Iwanaga, S., Namikawa, H. & Aoyama, S. (1972). J. Soc. Mat. Sci. Japan 21, 1106-1111.

Kelly, C. J., Short, M. A. and Evans, W. P. (1971). In Residual Stress Measurement by X-ray Diffraction, SAE Tech. Rep. J784a, pp. 60-65.

Kneer, G. (1965). Phys. Stat. Solidi 9, 825-838.

Krause, H. & Jühe, H. H. (1976). Härterei-Techn. Mitt. 31, 168-170.

Krause, H. & Jühe, H. H. (1977). Wear 36, 15-23.

Kröner, E. (1958). Z. Physik 151, 504-518.

Krŏner, E. (1967). J. Mech. Phys. Solid. 15, 319-329.

Lei, T. S. & Scardina, J. T. (1976). Microstructural Science, pp. 269-280. New York: Elsevier Publ. Co.

Lessells, J. M. & Broderick, R. F. (1956). Proc. Inter. Conf. on Fatigue of Metals, London, pp. 617-627.

Lode, W. & Peiter, A. (1977). Härterei-Techn. Mitt. 32, 235-240.

Macherauch, E. (1956). Z. Metallkde. 47, 312-330.

Macherauch, E. & Müller, P. (1961). Z. Angew Physik 13, 305-312.

Macherauch, E. & Wolstieg, U. (1977). Mater. Sci. & Eng. 30, 1-13.

Marion, R. H. & Cohen, J. B. (1975). Adv. in X-ray Analysis 18, 466-501.

Marion, R. H. & Cohen, J. B. (1977). Adv. in X-ray Analysis,20, 355-367.

Möller, H. and Martin, G. (1939). Mitteilungen K. W. I. Eisenforschg. Dusseldorf 21, 261-269.

Morris, P. R. (1970). Int. J. Eng. Sci. 8, 49-61.

Neerfeld, H. (1942). Mitteilungen K. W. I. Eisenforschg. Düsseldorf 24, 61-70.

Osswald, E. (1948). Z. Metallkde. 39, 279-288.

Peiter, A. (1976). Härterei-Tech. Mitt. 31, 158-165.

Peiter, A. & Lode, W. (1976). Metall. 30, 500-506.

Quesnel, D. J., Meshii, M. & Cohen, J. B. (1978). Mat. Sci. and Eng. 36, 207-215.

Reuss, A. (1929). Z. Angew. Math. u. Mech. 9, 49-58.

Schiebold, E. (1939). Berg.-u. Hüttenm. Monatsh. 86, 278-295.

Schreiber, E. (1976). Härterei-Techn. Mitt. 31, 86-89.

Shiraiwa, T. & Sakamoto, Y. (1970). The 13th Jap. Congr. on Mater. Res. Metal. Mater., Kyoto, Japan, 25-32.

Shiraiwa, T. and Sakamoto, Y. (1972). Sumitomo Search 7, 109-135.

Society of Automotive Engineers (1971). Residual Stress Measurement by X-ray Diffraction, SAE J784a. New York: Soc. Automotive Engineers, Inc.

Society of Materials Science, Japan (1973). Standard Method for X-ray Stress Measurement.

Stickforth, J. (1966). Techn. Mitt. Krupp Forsch.-Ber. 24, 89-102.

Taira, S., Hayashi, K. & Watase, Z. (1968). J. Soc. Mater. Sci., Japan 17, 1151-1157.

Voigt, W. (1928). Lehrbuch der Kristallphysik. Leipzig-Berlin: Teubner-Verlag.

Walburger, H. (1973). Conf. on Residual Stress Analysis, Starnberg, Germany.

Wecker, S. M. & Morris, P. R. (1978). J. Appl. Cryst. 11, 211-220.

Weidemann, W. (1966). Zur Versetzungsstruktur von plastisch verformtem α-Eisen. Ph.D. Thesis, Technische Hochschule Aachen, Germany.

Wolfstieg, U. (1976). Härterei-Techn. Mitt. 31, 19-22.

Wolfstieg, U. & Macherauch, E. (1976). Härterei-Techn. Mitt. 31, 83-85.

Table I: Possible Origins of Oscillations in d vs. $\sin^2\psi$

Authors	Bollenrath, Hauk and Weidemann (1967) Marion and Cohen (1975)	Peiter and Lode (1976)	Shiraiwa and Sakamoto (1970) Dölle and Hauk (1978)
Stress-State	Oscillation in stresses with φ and ψ due to local plastic response and texture	Superposition of strong gradients and shear residual stresses normal to the surface	Uniform or quasiuniform stresses as averages over the penetration depth of the X-ray beam*
Assumed Elasticity	Isotropic	Isotropic	Anisotropic
X-ray Elastic Constants Depending On	Reflection hkℓ, not φ and ψ	Reflection hkℓ, not φ and ψ	Reflection hkℓ and φ, ψ**

*Calculation for general multiaxial stress-states by Dölle and Hauk (1978).

**For h00 and hhh reflections the X-ray elastic constants do not depend on φ and ψ. (Dölle and Hauk, 1978).

Table II: Calculation of Bulk Elastic Constants by Statistical Theory of Elasticity

Author	Elastic Properties of Matrix	Elastic Properties of a Grain
Eshelby (1957, 1959)	Isotropic	Isotropic, but different from the elastic properties of the matrix
Krŏner (1958, 1967)	Isotropic	Anisotropic
Kneer (1965)	Anisotropic	Anisotropic with hexagonal symmetry (fiber-texture)
Morris (1970) Wecker and Morris (1978)	Anisotropic	Anisotropic with orthotropic symmetry (rolling texture)

Table III: Anisotropic X-ray Elastic Constants R'_{ij} and Stress Factors F_{ij} (Equation 42) for the 211-Reflection, Calculated for Preferred Orientations of α-iron (27) with an Isotropic Volume Fraction $\lambda_i = 0.2$.

Preferred orientation	λ_a	ψ_i	$\sin^2\psi_i$	ϕ_i	hkℓ	R'_{ij} in 10^{-6} MPa^{-1}						F_{ij} in 10^{-6} MPa^{-1}					
						R'_{11}	R'_{22}	R'_{33}	R'_{12}	R'_{13}	R'_{23}	F_{11}	F_{22}	F_{12}	F_{33}	F_{13}	F_{23}
		0.	0.	0.	211	-1.66	- .90	4.58	0.	0.	0.	-1.66	- .90	0.	4.58	0.	0.
				45.0	211	-1.28	-1.28	4.58	0.	0.	0.	-1.28	-1.28	0.	4.58	0.	0.
				90.0	211	- .90	-1.66	4.58	0.	0.	0.	- .90	-1.66	0.	4.58	0.	0.
(211)[01$\bar{1}$]	0,6			58.5	121	-1.10	-1.45	4.58	- .34	.92	- .56	- .12	.15	3.15	1.99	3.59	4.78
(211)[0$\bar{1}$1]		33.6	.306	121.5	112	-1.10	-1.45	4.58	.34	.92	.56	- .12	.15	-3.15	1.99	-3.59	4.78
				238.5	121	-1.10	-1.45	4.58	- .34	.92	- .56	- .12	.15	3.15	1.99	-3.59	-4.78
				301.5	112	-1.10	-1.45	4.58	.34	.92	.56	- .12	.15	-3.15	1.99	3.59	-4.78
				0	211	-1.01	-1.52	4.56	0.	.72	0.	.06	-1.52	0.	3.49	4.62	0.
				60.	112	-1.01	-1.52	4.56	0.	.72	0.	-1.13	- .34	1.37	3.49	2.31	4.00
(111)[$\bar{2}$11]	0,2	19.5	.111	120.	121	-1.01	-1.52	4.56	0.	.72	0.	-1.13	- .34	-1.37	3.49	-2.31	4.00
(111)[2$\bar{1}\bar{1}$]				180.	211	-1.01	-1.52	4.56	0.	.72	0.	.06	-1.52	0.	3.49	-4.62	0.
				240.	112	-1.01	-1.52	4.56	0.	.72	0.	-1.13	- .34	1.37	3.49	-2.31	-4.00
				300.	121	-1.01	-1.52	4.56	0.	.72	0.	-1.13	- .34	-1.37	3.49	2.31	-4.00
				0.	211	-1.01	-1.52	4.56	0.	-.72	0.	.17	-1.52	0.	3.38	4.77	0.
				90.	2$\bar{1}$1	-1.01	-1.52	4.56	0.	-.72	0.	-1.52	.17	0.	3.38	0.	4.77
(100)[011]	0,2	35.3	.333	180.	2$\bar{1}\bar{1}$	-1.01	-1.52	4.56	0.	-.72	0.	.17	-1.52	0.	3.38	-4.77	0
				270.	21$\bar{1}$	-1.01	-1.52	4.56	0.	-.72	0.	-1.52	.17	0.	3.38	0.	-4.77

Table III (Continued for the 310-Reflection)

Preferred orientation	λ_a	ψ_i	$\sin^2\psi_i$	ϕ_i	hkℓ	R'_{ij} in 10^{-6} MPa^{-1}						F_{ij} in 10^{-6} MPa^{-1}					
						R'_{11}	R'_{22}	R'_{33}	R'_{12}	R'_{13}	R'_{23}	F_{11}	F_{22}	F_{12}	F_{33}	F_{13}	F_{23}
				58.5	301	-2.45	-1.77	6.24	.24	.33	1.05	-2.04	- .33	.45	4.39	2.29	6.97
(211)[01$\bar{1}$]	0,6	25.4	.183	121.5	310	-2.45	-1.77	6.24	-.24	.33	-1.05	-2.04	- .33	- .45	4.39	-2.29	6.97
(211)[0$\bar{1}$1]				238.5	301	-2.45	-1.77	6.24	.24	.33	1.05	-2.04	- .33	.45	4.39	-2.29	-6.97
				301.5	310	-2.45	-1.77	6.24	-.24	.33	-1.05	-2.04	- .33	- .45	4.39	2.29	-6.97
				19.1	310	-2.07	-1.84	5.93	-.25	.39	-.62	2.01	-1.80	1.46	1.81	7.78	2.10
				40.9	013	-2.07	-1.84	5.93	.25	.39	.62	- .21.	.43	4.02	1.81	5.71	5.69
				79.1	103	-2.07	-1.84	5.93	-.25	.39	-.62	-1.48	1.69	2.56	1.81	2.07	7.79
				100.9	130	-2.07	-1.84	5.93	.25	.39	.62	-1.48	1.69	-2.56	1.81	-2.07	7.79
				139.1	031	-2.07	-1.84	5.93	-.25	.39	-.62	- .21	.43	-4.02	1.81	-5.71	5.69
(111)[$\bar{2}$11]	0.2	43.1	.467	160.9	301	-2.07	-1.84	5.93	.25	.39	.62	2.01	-1.80	-1.46	1.81	-7.78	2.10
(111)[2$\bar{1}\bar{1}$]				199.1	310	-2.07	-1.84	5.93	-.25	.39	-.62	2.01	-1.80	1.46	1.81	-7.78	-2.10
				220.9	013	-2.07	-1.84	5.93	.25	.39	.62	- .21	.43	4.02	1.81	-5.71	-5.69
				259.1	103	-2.07	-1.84	5.93	-.25	.39	-.62	-1.48	1.69	2.56	1.81	-2.07	-7.79
				280.9	130	-2.07	-1.84	5.93	.25	.39	.62	-1.48	1.69	-2.56	1.81	2.07	-7.79
				319.1	031	-2.07	-1.84	5.93	-.25	.39	-.62	- .21	.43	-4.02	1.81	5.71	-5.69
				340.9	301	-2.07	-1.84	5.93	.25	.39	.62	2.01	-1.80	-1.46	1.81	7.78	-2.10
				45.0	301	-1.68	-2.23	5.93	0.	- .73	0.	-1.80	-1.80	.87	5.61	2.40	2.40
(100)[011]	0.2	18.4	.100	135.0	3$\bar{1}$0	-1.68	-2.23	5.93	0.	- .73	0.	-1.80	-1.80	- .87	5.61	-2.40	2.40
				225.0	30$\bar{1}$	-1.68	-2.23	5.93	0.	- .73	0.	-1.80	-1.80	.87	5.61	-2.40	-2.40
				215.0	310	-1.68	-2.23	5.93	0.	- .73	0.	-1.80	-1.80	- .87	5.61	2.40	-2.40

Fig. 1 Definition of the angles φ and ψ and orientation of the laboratory-system $\underline{L}_i$ with respect to the sample system $\underline{P}_i$.

Fig. 2 Nonlinear lattice-strain distributions vs. $\sin^2\psi$

a. after deformation by tangent stresses

b. after cold rolling

Fig. 3 Isotropic X-ray elastic constants for iron vs. 3Γ, calculated in Voigt, Reuss and Eshelby-Kröner limit.

Fig. 4 Lattice strain vs. $\sin^2\psi$ measured (Dölle and Cohen, in press), in a ground steel (C:0.6%; Si:0.25%; Mn:0.75%).

Measured values: ● $\psi \geq 0$; ○ $\psi < 0$.

——— Calculated from stress tensor (25).

------ Average strain a_1 (23a).

Fig. 5 Poles for the {211} and {310} planes, calculated for the preferred orientations of α-iron (27). The length of the radius-vector is $\sin^2\psi$.

Fig. 6 Experimental X-ray elastic constants R'_{11} (211, ψ=0, ζ) (according to Dölle, Hauk and Zegers, 1978) for the preferred orientation (211)[$0\bar{1}\bar{1}$] or [$0\bar{1}1$]; measured in cold rolled steels (C:0.10%; Si:0.34%; Mn:1.34%) at various directions $\varphi = \zeta$. Reduction: ○ 30%; □ 50%; △ 75%.

The isotropic and anisotropic limits have been calculated from equation (26).

Fig. 7 Lattice strain ε'_{33} vs. $\sin^2\psi$ calculated for quasi-isotropic (------) and for textured (●) iron having the preferred orientations (27). A stress of 100 MPa has been assumed to be parallel to the cut out direction ζ. ψ^{**} are

texture independent directions (Hauk and Sesemann, 1976)

Fig. 8 Influence of transverse stresses σ_{22} on lattice strain distributions in quasi-isotropic (upper diagrams) and textured iron.

Fig. 9 Influence of stress gradients g_{ij} on d vs. $\sin^2\psi$. $\langle\sigma_{11}\rangle$ and $\langle\sigma_{33}\rangle$ are averages over the penetration depth of the X-ray beam (equation 52). Note that $\sigma_{33}(2=0) = 0$.

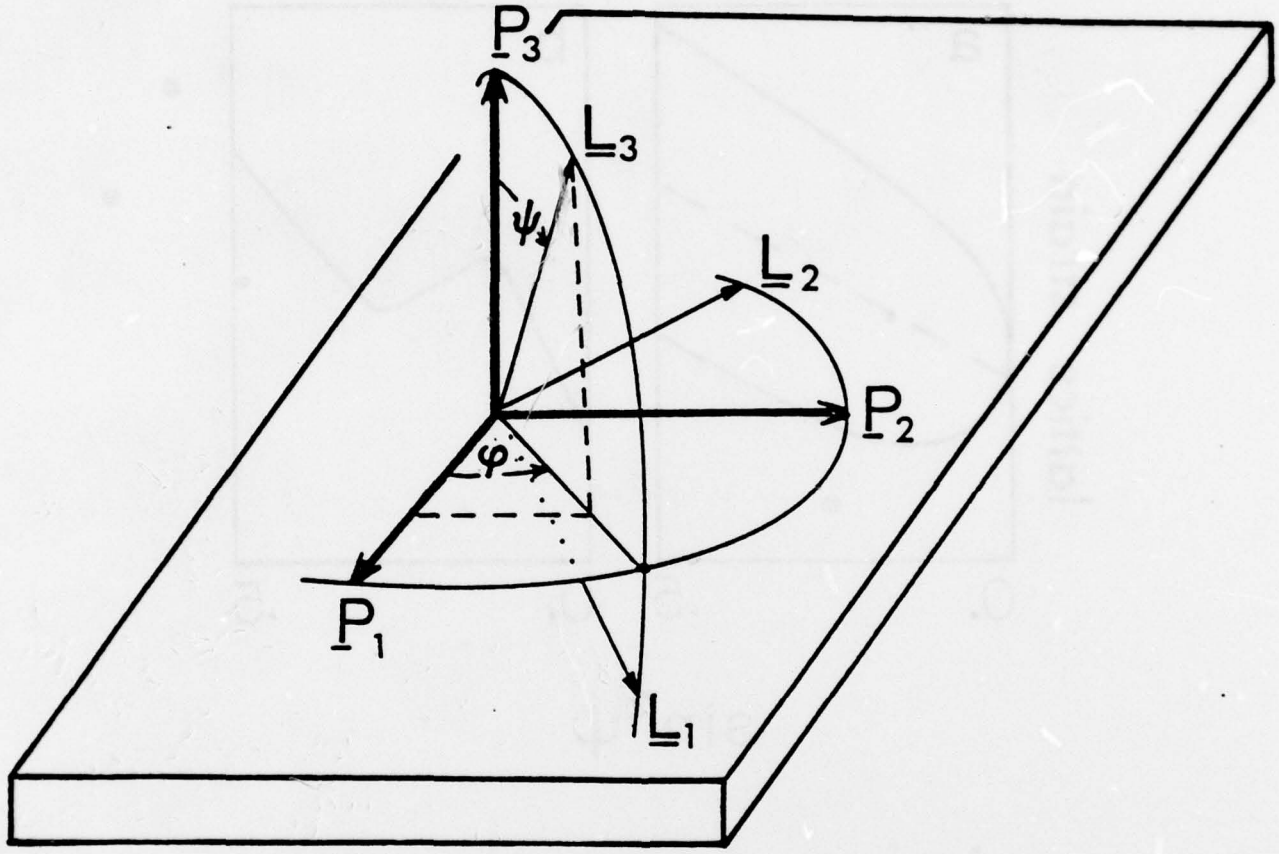

fig. 1

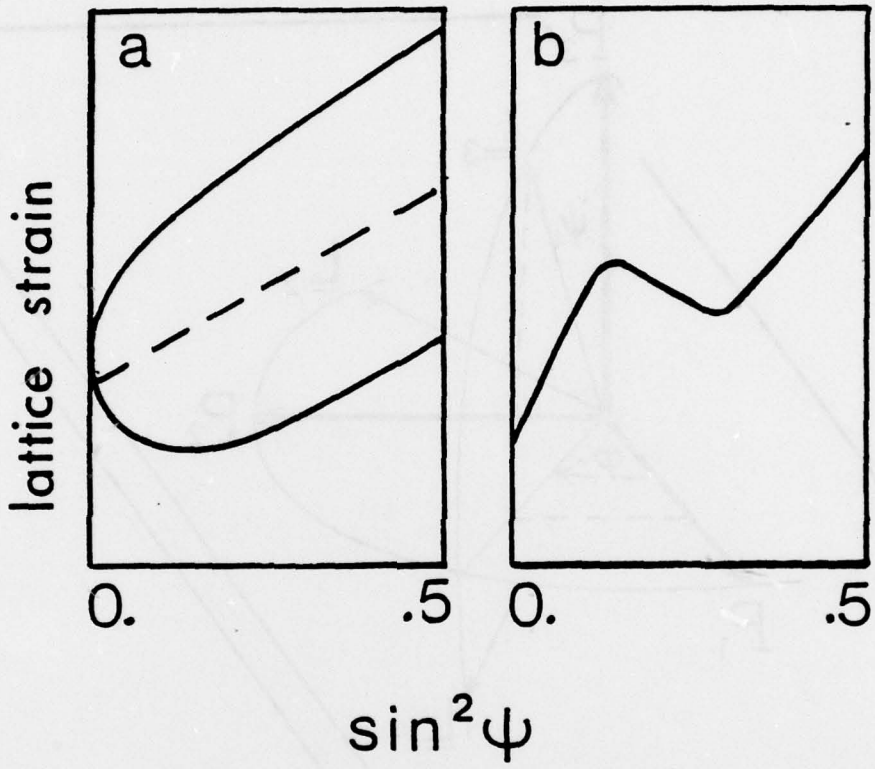

fig. 2

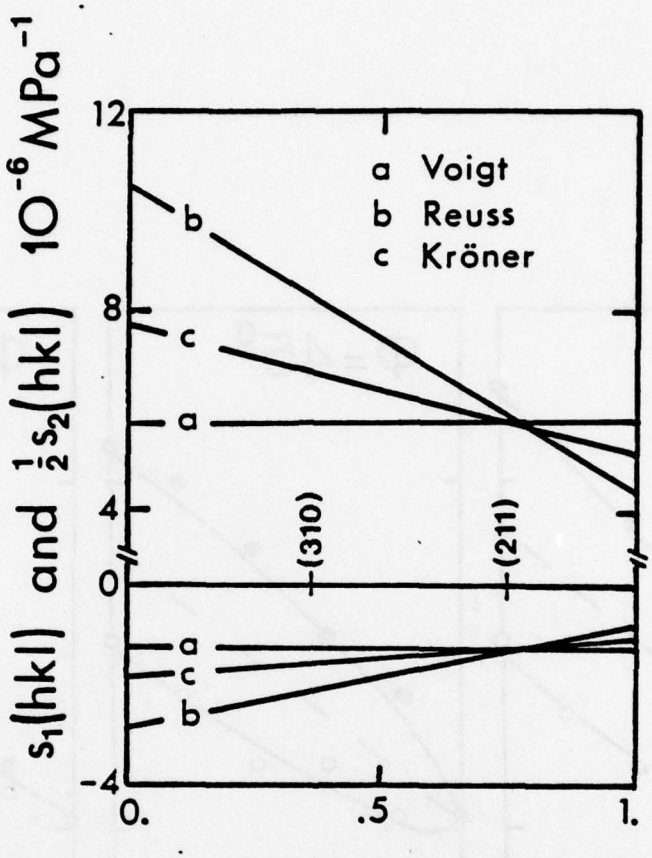
$s_1(hkl)$ and $\frac{1}{2}s_2(hkl)$ 10^{-6} MPa^{-1}
12
8
4
0
-4
0.
.5
1.
a Voigt
b Reuss
c Kröner
a
b
c
(310)
(211)
a
c
b

3Γ

fig. 3

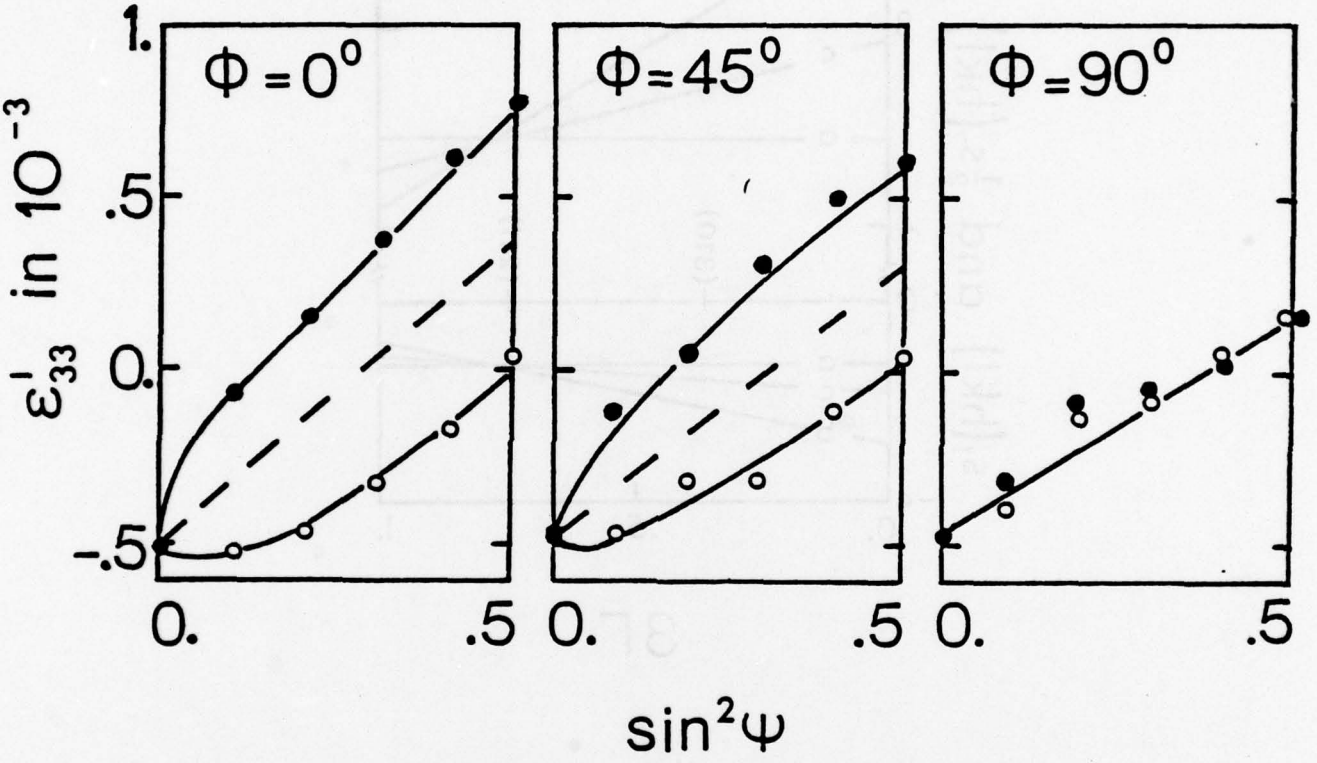

fig. 4

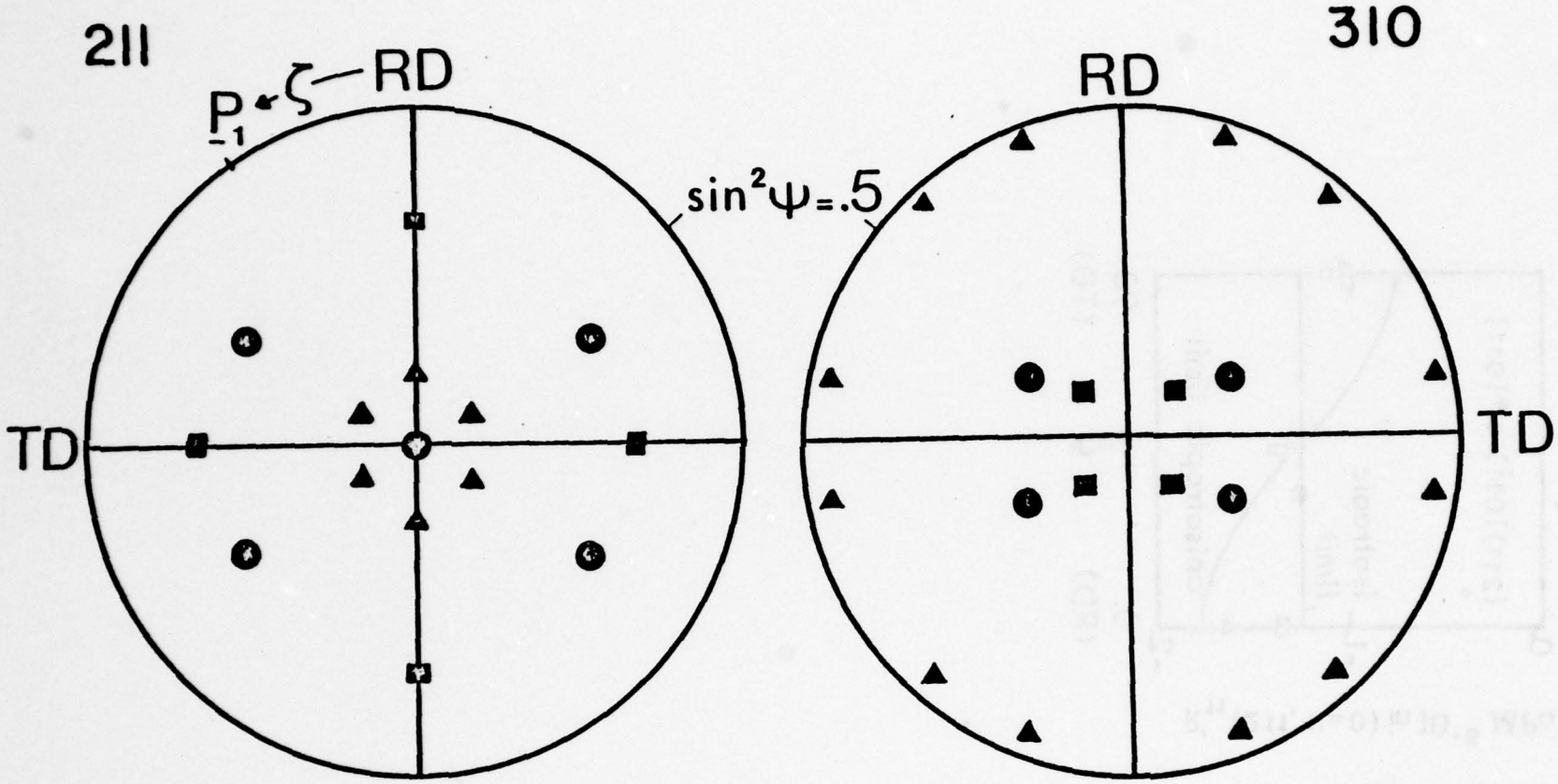

Preferred Orientations: ● (211)[01$\bar{1}$] or [0$\bar{1}$1]

■ (100)[011]

▲ (111)[$\bar{2}$11] or [2$\bar{1}\bar{1}$]

fig. 5

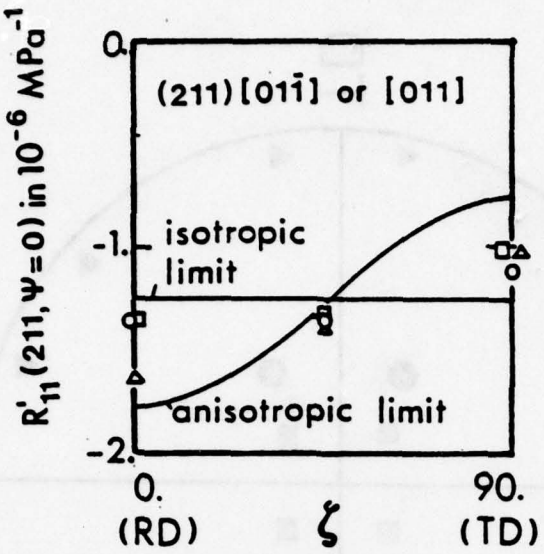
0.
(211)[01$\bar{1}$] or [011]
-1.
isotropic
limit
anisotropic limit
-2.
0.
(RD)
ζ
90.
(TD)
$R'_{11}(211, \Psi=0)$ in 10^{-6} MPa^{-1}

fig. 6

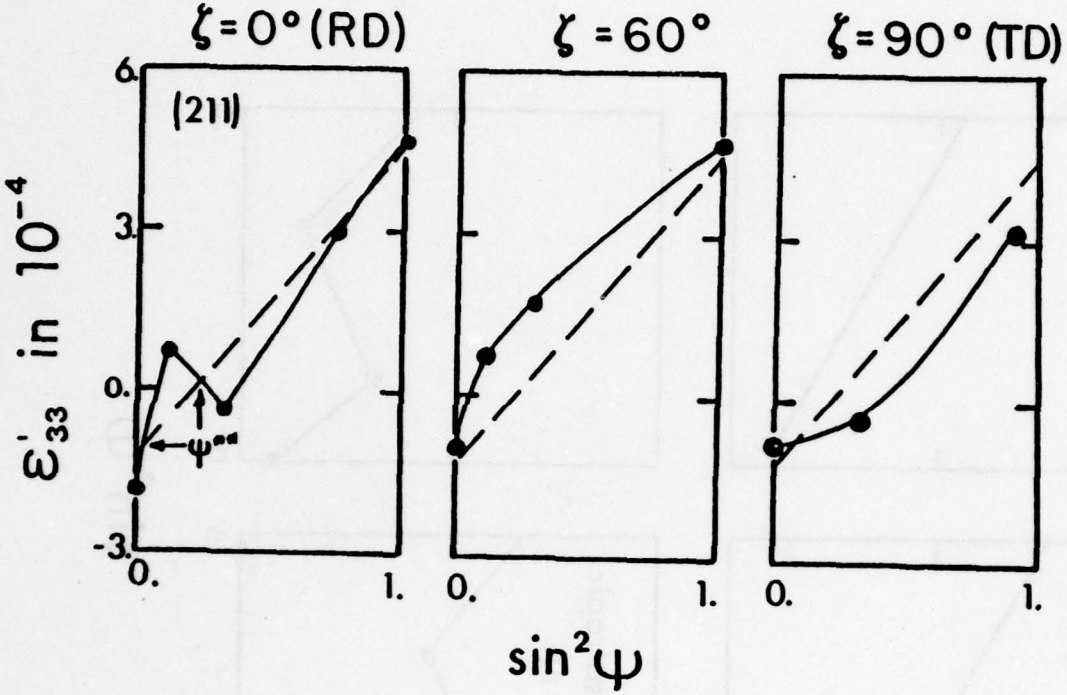
ζ = 0° (RD)
ζ = 60°
ζ = 90° (TD)
(211)
6.
3.
0.
-3.
0.
1.
ε'_{33} in 10^{-4}
ψ^{max}
$\sin^2\psi$

fig. 7

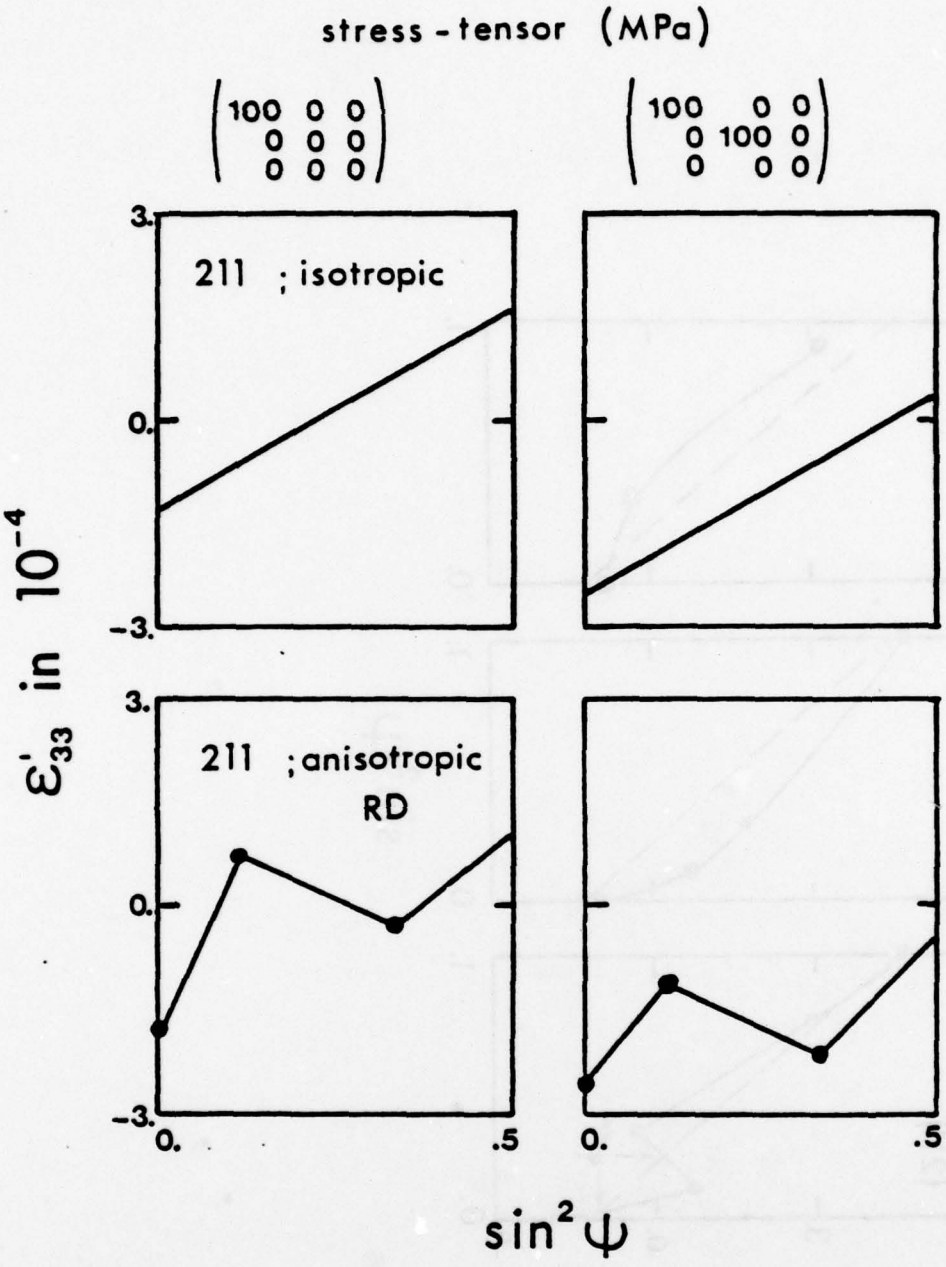
stress - tensor (MPa)
100 0 0
0 0 0
0 0 0
100 0 0
0 100 0
0 0 0
211 ; isotropic
211 ; anisotropic
RD
3.
0.
-3.
0.
.5
ε'_{33} in 10^{-4}
$\sin^2\psi$

fig. 8

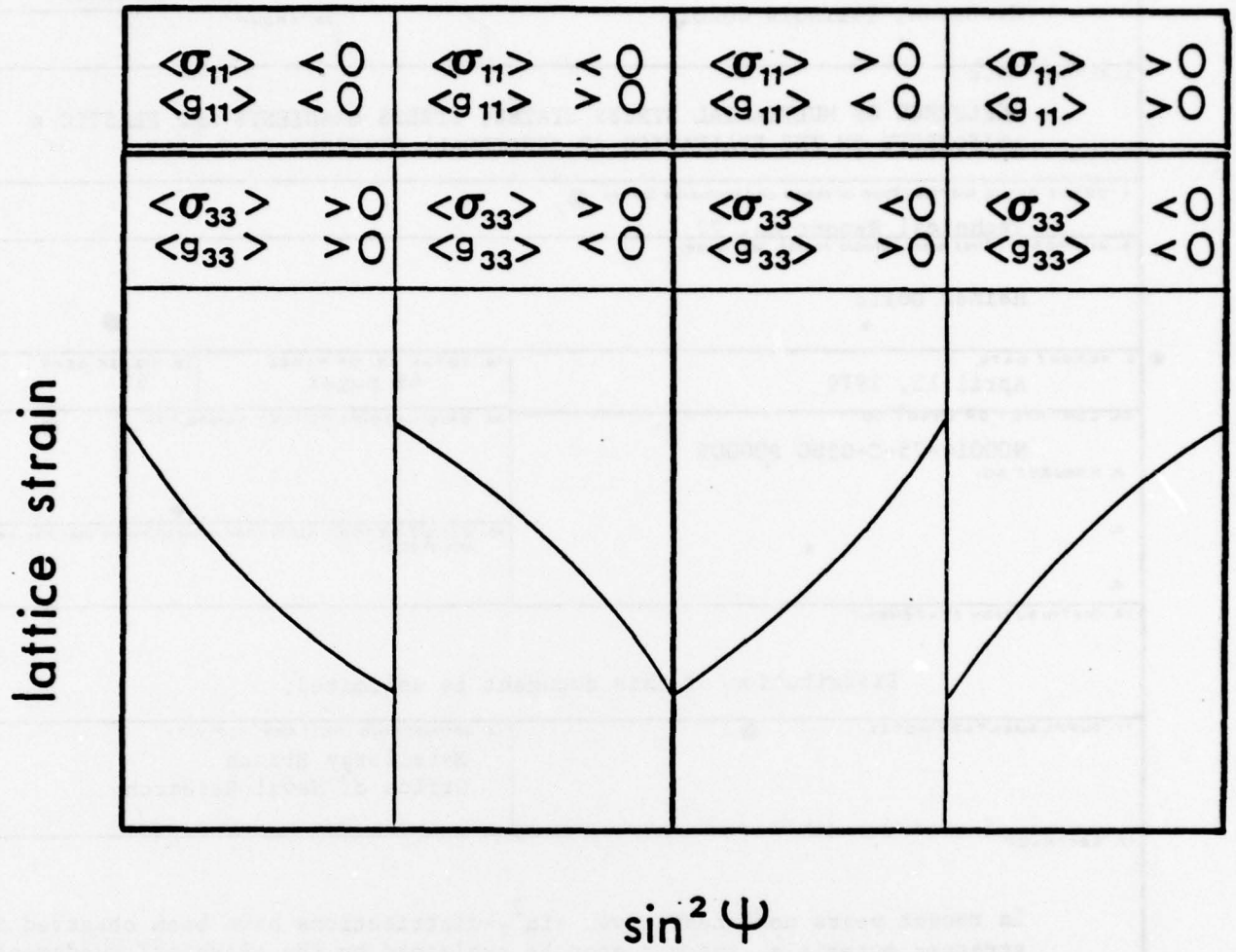
$\langle\sigma_{11}\rangle < 0$
$\langle g_{11}\rangle < 0$
$\langle\sigma_{11}\rangle < 0$
$\langle g_{11}\rangle > 0$
$\langle\sigma_{11}\rangle > 0$
$\langle g_{11}\rangle < 0$
$\langle\sigma_{11}\rangle > 0$
$\langle g_{11}\rangle > 0$
$\langle\sigma_{33}\rangle > 0$
$\langle g_{33}\rangle > 0$
$\langle\sigma_{33}\rangle > 0$
$\langle g_{33}\rangle < 0$
$\langle\sigma_{33}\rangle < 0$
$\langle g_{33}\rangle > 0$
$\langle\sigma_{33}\rangle < 0$
$\langle g_{33}\rangle < 0$
lattice strain
$\sin^2\Psi$

fig. 9

Security Classification

DOCUMENT CONTROL DATA - R & D

Security classification of title, body of abstract and indexing annotation must be entered when the overall report is classified)

1. ORIGINATING ACTIVITY (Corporate author) H. Dölle, Northwestern University, Evanston, Illinois 60201	2a. REPORT SECURITY CLASSIFICATION Unclassified 2b. GROUP

3. REPORT TITLE

INFLUENCE OF MULTIAXIAL STRESS STATES, STRESS GRADIENTS AND ELASTIC ANISOTROPY ON THE EVALUATION OF (RESIDUAL) STRESSES BY X-RAYS

4. DESCRIPTIVE NOTES (Type of report and inclusive dates)

Technical Report No. 22

5. AUTHOR(S) (First name, middle initial, last name)

Heiner Dölle

6. REPORT DATE April 12, 1979	7a. TOTAL NO. OF PAGES 49 pages	7b. NO. OF REFS 63
8a. CONTRACT OR GRANT NO. N00014-75-C-0580 P00005 b. PROJECT NO. c. d.	9a. ORIGINATOR'S REPORT NUMBER(S) 9b. OTHER REPORT NO(S) (Any other numbers that may be assigned this report)	

10. DISTRIBUTION STATEMENT

Distribution of this document is unlimited.

11. SUPPLEMENTARY NOTES	12. SPONSORING MILITARY ACTIVITY Metallurgy Branch Office of Naval Research

13. ABSTRACT

In recent years nonlinear d vs. $\sin^2\psi$-distributions have been observed in stressed materials, which cannot be explained by the classical fundamentals of X-ray stress measurement. d- is the interplanar spacing measured and ψ is the angle between the surface normal of the sample and the measuring direction. This paper reviews treatments for these nonlinear distibutions, including stress gradients, shear-stresses and anisotropic X-ray elastic constants. Methods for the evaluation of stresses are reported, and recommendations are given for the practical application of X-ray stress measurement.

DD FORM 1 NOV 68 1473 (PAGE 1)

S/N 0101-807-6801

Security Classification

14. KEY WORDS	LINK A		LINK B		LINK C	
	ROLE	WT	ROLE	WT	ROLE	WT
residual stresses, stresses, X-rays, diffraction						